FIRST-PRINCIPLES STUDY OF STRUCTURAL, ELECTRONIC AND MAGNETIC PROPERTIES OF DEFECTED (MONOVACANT) HEXAGONAL BORON NITRIDE SHEET

A Dissertation

Submitted to the Central Department of Physics, Tribhuvan University, Kirtipur in the Partial Fulfillment for the Requirement of Master's Degree of Science in Physics

By

Kisan Khatri

Symbol No : 1549/073

Reg. No : 5-2-50-902-2012

March, 2021

RECOMMENDATION

It is certified that Mr. Kisan Khatri has carried out the dissertation work entitled "**FIRST-PRINCIPLES STUDY OF STRUCTURAL, ELECTRONIC AND MAGNETIC PROPERTIES OF DEFECTED (MONOVACANT) HEXAGONAL BORON NITRIDE SHEET** " under my supervision and guidance.

I recommend the dissertation in the partial fulfillment for the Master's Degree of Science in Physics.

Nurapati

(Supervisor)

Dr. Nurapati Pantha

Associate Professor

Central Department of Physics

Tribhuvan University, Kirtipur

Kathmandu, Nepal

Date: 2021|03|14

ACKNOWLEDGEMENT

I would like to extend my heartfelt appreciation to all the helping hands that have supported me throughout my thesis. I would not have been able to finish this job without their assistance.

It provides me tremendous joy to extend my deep feeling of indebtedness and deep appreciation to my renowned supervisor Dr. Nurapati Pantha, for his expert advice, periodic oversight and continuous assistance throughout my study job. I was helped by his continuous guidance and persistent encouragement to produce a fruitful study of this job.

I am thankful to Prof. Dr. Om Prakash Niraula (Head, Central Department of Physics) for his valuable contributions for this work and also for his encouragement and motivation for the successful life .

My sincere thanks and deep gratitude goes to Prof. Dr. Narayan Prasad Adhikari for his regular encouragement, support and guidance throughout this work as well as to my life .

I am always grateful to Prof. Dr. Binil Aryal (former Head, Central Department of Physics) for his regular inspiration and support throughout the M.Sc. journey as well as to my life.

Additionally, I am grateful to all the respected faculties and entire family of Central Department of Physics.

I would like to thank elders, my friends and all the other peers with whom I spent important hours during my dissertation.

My acknowledgement also goes through the Master's Thesis Support program to the University Grants Commission and Gaumukhi Rural Municipality for their partial economic support.

I am also thankful to respected sir H. K. Neupane sir and friend Kamal Khanal for their help and support throughout this work.

Last but not least, for their love, patience and constant support, I would like to dedicate this thesis to my family members that made it possible for me to join this field of scientific research despite many hardships.

EVALUATION

We certify that we have read this dissertation and in our opinion, it is good in the scope and quality as dissertation in partial fulfillment for the requirement of Master's Degree of Science in Physics.

Evaluation committee

Nurapati

Dr. Nurapati Pantha
(supervisor)
Associate Professor
Central Department of Physics
Tribhuvan University, Kirtipur
Kathmandu, Nepal

O. P. Niraula

(Prof. Dr. Om Prakash Niraula)
(Head)
Central Department of Physics
Tribhuvan University, Kirtipur
Kathmandu, Nepal

(External Examiner)

Narayan

(Internal Examiner)

Date: 2021/03/17

Abstract

The first-principles calculations based GGA functionals was implemented to study the structural, electronic and magnetic properties of pure and defected hexagonal boron nitride (h-BN) monolayer sheet using Quantum ESPRESSO (QE) package, 6.5 version. The pure h-BN is found to be non-magnetic insulator with band gap of 4.64 eV. The calculated values of formation energy reveals the structural stability of defected system. The formation energies for B and N vacant system are found to be 16.45 eV and 12.84 eV respectively which predicts that N vacant system is more preferable with lower formation energy. The defect on a system abruptly changes the electronic and magnetic properties of h-BN system. The 6.25 % B-vacancy and 6.25 % N-Vacancy defects are found to be half metallic ferromagnet with total magnetization of $2.74\mu_B$/cell and magnetic semiconductor with total magnetization $1.00\mu_B$ /cell respectively.

List of Abbreviations

h-BN: Hexagonal Boron Nitride

V_B : Single Boron Vacancy

V_N : Single Nitrogen Vacancy

NT : Nano Tube

PWscf : Plane Wave self-consistent field

DFT : Density Functional Theory

PAW : Projector Augmented Wave

GGA : Generalized Gradient Approximation

DOS : Density of States

ESPRESSO: opEn-Source Package for Research in Electronic Structure, Simulation, and Optimization

SCF : Self Consistent Field

HK :Hohenberg-Kohn

HF : Hartee-Fock

KS : Kohn-Sham

LSDA : Local Spin Density Approximation

LDA : Local Density Approximation

XC : Exchange and Correlation

List of Figures

List of Tables

Contents

Chapter 1

Introduction

1.1 General Consideration

The study of crystalline materials have been doing since long. Discovery of graphene in 2004 and its astonishing properties have given birth to a new class of materials known as two dimensional (2D) materials like phosphorene, hexagonal Boron Nitride, silicene, stanene, transition metal di-chalcogenides (TMDCs) etc [1]. Intense studies in such materials are growing these days. In our work, we have studied the different properties of defected (monovacant) two dimensional hexagonal Boron Nitride.

1.1.1 Crystal Defect

Crystal defect is the imperfection in the regular geometrical arrangement of the atoms in a crystalline solid. A crystal is never perfect; a variety of imperfections can mar the ordering. A defect is a small imperfection affecting a few atoms. The simplest type of defect is a missing atom and is called a vacancy [2]. Defects are essential for a crystalline solid to be in thermal equilibrium. Defects are called surface, line, or point defects, according to whether the imperfect region is bounded on the atomic scale in one, two or three dimensions [3]. Point defects include vacancies, interstitial atoms, impurity atoms and their combinations. Line defects are lines along which whole rows of atoms in a solid are arranged anomalously; also called dislocation. Two-dimensional defects include grain boundaries, stacking factors etc. whereas three dimensional defects involve holes, inclusions, precipitates etc [4]. In our work we have analysed the structural, electronic and magnetic properties of hexagonal Boron Nitride due to the effect of single vacancy.The following figure shows the Schottky defect and Frenkel defect. In schottky defect vacancy is created due to the excitation of atom or ion from the interior of the

crystal and in frenkel defect but in this case atom resides to the interior of the crystal creating vacancy.

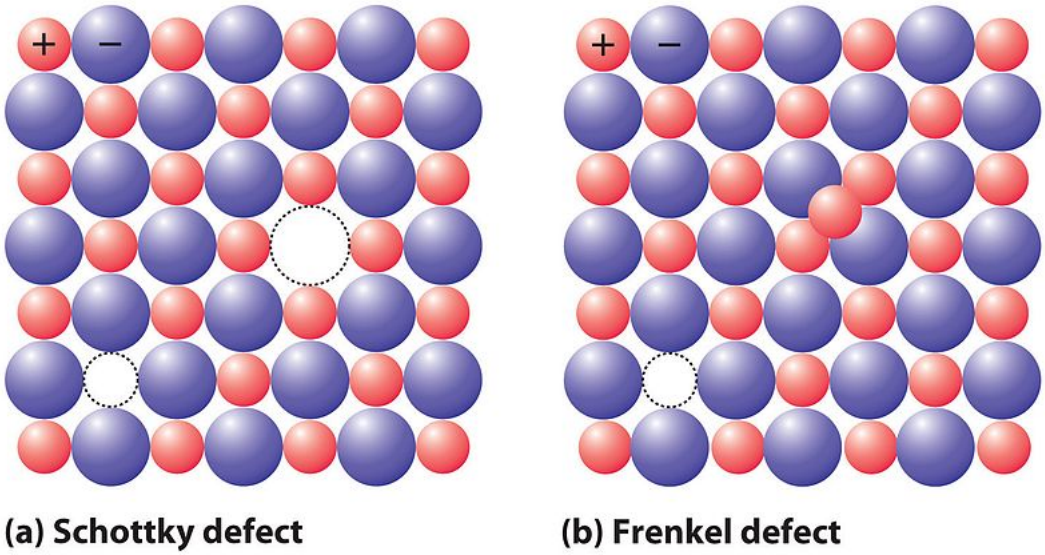

Figure 1.1: Schottky defect and Frenkel defect

1.1.2 Boron Nitride (BN)

Boron nitride is a heat and chemically resistant refractory compound of boron and nitrogen with the chemical formula BN. It is a modern man made compound that perfectly parallels the crystalline structure and properties of naturally occurring elementary carbon [5] . It has potential use in nanotechnology. The structural analogue of a carbon nanotube (CNT), a BN nanotube (BNNT) was first predicted in 1994; since then, it has become one of the most intriguing non-carbon nanotubes [6]. Hexagonal Boron Nitride, cubic Boron Nitride, amorphous Boron Nitride and Wurtzite form of Boron Nitride are the different crystalline forms of BN that are isoelectronic to a similarly structured carbon lattice. Hexagonal Boron Nitride is one of the known representative crystal structure of BN.

1.1.3 Hexagonal Boron Nitride (h-BN)

After the discovery of graphene, hexagonal Boron Nitride was first discovered in 2005. It has similar bonding and structure to graphite which is also called white graphene. It is comprised of alternating boron and nitrogen atoms in a honeycomb arrangement, consisting of sp^2-bonded two-dimensional layers in which Boron and Nitrogen atoms are bounded by strong covalent bonds within each layer of hexagonal BN whereas the

layers are held together by weak van der Waals forces [7]. Hexagonal boron nitride has a similar two-dimensional structure with a distinct chemical species and exhibits completely different physical properties from graphene. In order to clarify the lattice defects in h-BN such as vacancies or edges, the individual boron and nitrogen atoms should be directly imaged and even distinguished; otherwise the precise defect structures cannot be deduced [8] . The interlayer spacing of h-BN is 0.33 nm which is slightly less than that of the graphite (0.335 nm) in which B-N bond length is $1.45A^o$ which forms through sp^2 hybridization [9]. As an insulating material with a band gap of 5.97 eV, h-BN has an atomically flat surface, a very low roughness, no dangling bonds on its surface, and in combination with graphene shows weak van der Waals force, a minimal impact on graphite dilute carrier transport properties, a mismatch of 1.84 % with the graphene lattice and has no doping effect on graphene [9]. The unit cell parameters for h-BN are a = b = $2.50 - 2.51A^o$, c = $6.66 - 6.67A^o$, $\alpha = \beta = 90°$, $\gamma = 120$ ° [10]. Low-dimensional h-BN possess copious physical properties whereas its epitaxial layers show excellent semiconducting properties and h-BN is the nominating material for deep ultraviolet (DUV) photoelectronic devices [11]. Due to stupefying properties of h-BN, it has wide applications in micro and nanodevices such as insulator with high thermal conductivity in electronic appliances.

Hexagonal boron nitride sometimes regarded as a white graphite but it is more stable than graphite [12]. In bulk h-BN the lattice constants are a_0=b_0= 2.51 Å and c= 6.66 Å [13]. Although 2D h-BN has a fascinating properties, the subject of the band gap is always an interesting topic for all. Since the band gap value and it's nature for h-BN is not unique and it precisely depends on the number of techniques employed for it's determination. There are some techniques that gives the direct band gap and some shows that the band gap is indirect. From literature we find that the range of band gap of h-BN from 3.0 to 7.5 eV [14].

1.1.4 Monolayer h-BN

Monolayer h-BN has been isolated from bulk BN and could be useful as a complementary two-dimensional dielectric substrate for graphene electronics. It is structurallly similar to graphene also known as white graphene [7]. The bond is sp^2 hybridised and it's length is $1.446A^o$ [9]. Theoretically the thermal conductivity of monolayer 2D h-BN is expected to be more than $600Wm^{-1}K^{-1}$ as that of bulk h-BN can reach $400Wm^{-1}K^{-1}$ at room temperature. The young's modulus of monolayer h-BN is 0.71-0.97 TPa [15]. It is chemically and thermally stable which has promising semiconducting characteristics.

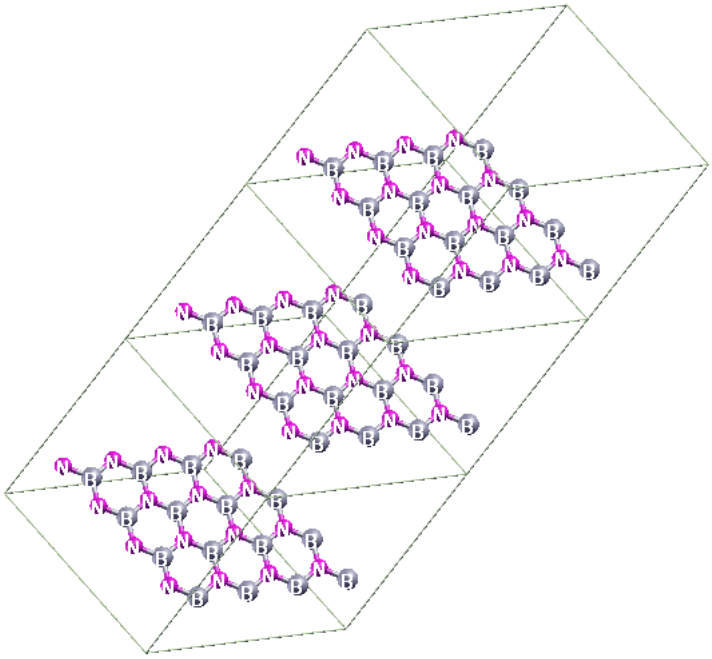

Figure 1.2: Layered h-BN

1.2 Scope of The Present Work

In our work, first- Principle calculation has been performed using DFT calculations with GGA for exchange-correlation energy implemented in Quantum-ESPRESSO package to study the stability, geometrical structures, electronic and magnetic properties of pristine hexagonal boron nitride (h-BN) as well as monovacant (Boron and Nitrogen vacancy) h-BN system in two dimensions(2D).
The main objectives of this research work are:

- To study the stability and energy of pure and single vacant hBN.
- To study the band structural properties of pristine and single vacant hBN.
- To study the structural, magnetic and electronic properties of pristine hBN and single vacant hBN.

In the second chapter, we will start from the discussion of Many body Hamiltonian as well as the theoretical developments significant to solve many-body problem and underlines the importance of DFT as first-principles calculations.

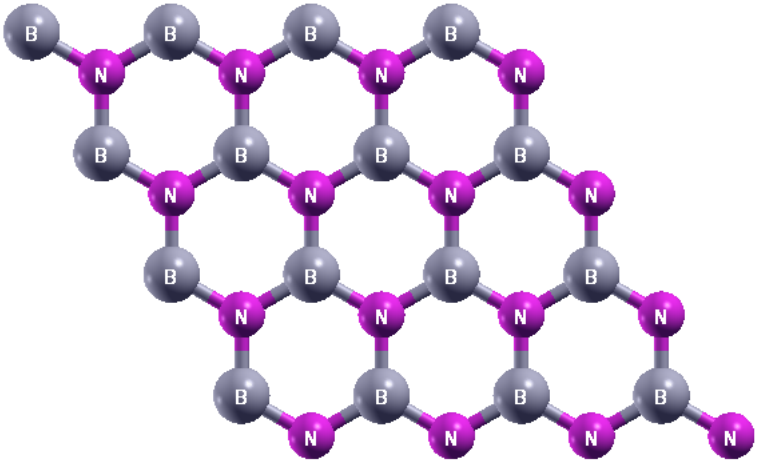

Figure 1.3: Vertical view of 4x4 supercell of monolayer h-BN

In chapter three, we discuss about the simulation details of our first-principle calculations under DFT using Quantum ESPRESSO package. In chapter four, we include the main findings of our present work where we analyze the findings and provide the reasons behind them. This chapter contains the answers we are looking for or the main purpose of our queries, with band structure and DOS calculations of the system under investigation. Finally in chapter five, we take a glimpse of the work we performed and put forth the scope of further research in the same system.

Chapter 2

Theoretical Background

2.1 Schrödinger equation and many-body Hamiltonian :

The study of effects of defects in the system makes a many body problem of quantum mechanics. Consider a many body system consisting of M nuclei and N electrons. We use the time-independent and non-relativistic schrödinger equation to describe this system as

$$\begin{aligned}\hat{\mathrm{H}}_i(\vec{x}_1, \vec{x}_2, ..., \vec{x}_N, \vec{R}_1, \vec{R}_2, ..., \vec{R}_M)\Psi_i(\vec{x}_1, \vec{x}_2, ..., \vec{x}_N, \vec{R}_1, \vec{R}_2, ..., \vec{R}_M) \\ = E_i\Psi_i(\vec{x}_1, \vec{x}_2, ..., \vec{x}_N, \vec{R}_1, \vec{R}_2, ..., \vec{R}_M)\end{aligned} \tag{2.1}$$

Here $\hat{\mathrm{H}}$ is a Hamilton operator of a system of N electrons and M nuclei. The expression for this hamiltonian is given by,

$$\hat{\mathrm{H}} = -\frac{\hbar^2}{2m_e}\sum_{i=1}^{N}\nabla_i^2 - \frac{\hbar^2}{2M_j}\sum_{j=1}^{M}\nabla_j^2 - \sum_{i=1}^{N}\sum_{j=1}^{M}\frac{Z_j e^2}{|\vec{r}_i - \vec{R}_j|} + \sum_{i=1}^{N}\sum_{j>i}^{N}\frac{e^2}{|\vec{r}_{ij}|} + \sum_{i=1}^{M}\sum_{j>i}^{M}\frac{Z_i Z_j e^2}{|\vec{R}_{ij}|} \tag{2.2}$$

In above equation Many body hamilton, the first and second terms are the expression for the kinetic energy of N electrons and M nuclei respectively where as the last three terms are the expression for potential energy. Among three last term , the third term is the coulomb interaction between electron and nuclei which is attractive in nature while the fourth and the fifth term are the electron-electron and nuclei-nuclei interaction and are repulsive in nature. Here m_e is the mass of electron and M_j is mass of j^{th} nucleus. Also, $\mathrm{r}_{ij} = |\vec{r_i} - \vec{r_j}|$. Also, the wave function $\Psi_i(\vec{x}_1, \vec{x}_2, ..., \vec{x}_N, \vec{R}_1, \vec{R}_2, ..., \vec{R}_M)$ depends on 3N spacial coordinates $\{\vec{r_i}\}$, and N spin coordinates $\{\alpha_i\}$ of electrons. They are collectively termed $\{\vec{x}_i\}$ and 3M spatial coordinates of the nuclei, $\{\vec{R}_j\}$. It is well

known that we can obtain all the information about quantum system if we know the wave function Ψ_i of that system. Also the energy eigenvalue is E_i for ith state of system. We can simplify the Schrödinger equation by using ***Born-Oppenheimer*** approximation. Since, nuclei are much more heavier than electrons. More precisely, Each proton is almost 1800 times heavier than electron. This implies that the motion of nuclei are very slow in comparison to the motion of electron. Hence, we neglect the motion of nuclei and assume that electrons moving in the field of a set of fixed nuclei which is exactly we called ***Born-Oppenheimer*** approximation. By employing this approximation we can solve Schrödinger equation only for electrons. The kinetic energy of nucleus is zero due to their fixed position and the potential energy caused by nuclei-nuclei repulsive interactions is a constant. Hence, Hamiltonian of equation becomes electronic hamiltonian as

$$\begin{aligned}\hat{\mathrm{H}}_{elec} &= -\frac{\hbar^2}{2m_e}\sum_{i=1}^{N}\nabla_i^2 - \sum_{i=1}^{N}\sum_{j=1}^{M}\frac{Z_j e^2}{\vec{r}_i - \vec{R}_j} + \sum_{i=1}^{N}\sum_{j>i}^{N}\frac{e^2}{\vec{r}_{ij}} \\ &= \hat{\mathrm{T}} + \hat{\mathrm{V}}_{Ne} + \hat{\mathrm{V}}_{ee}.\end{aligned} \tag{2.3}$$

Now, we can obtain the energy E_{elec} and the wave function Ψ_{elec} by solving the Schrödinger equation

$$\hat{\mathrm{H}}_{elec}\Psi_{elec} = E_{elec}\Psi_{elec} \tag{2.4}$$

Now the total energy E_{total} can be written as the sum of electronic energy E_{elec} and the energy of the nucleus which will be constant nuclei-nuclei repulsive interaction E_{nuc}.

$$\begin{aligned}E_{tot} &= E_{elec} + \sum_{i=1}^{M}\sum_{j>i}^{M}\frac{Z_i Z_j e^2}{R_{ij}} \\ &= E_{elec} + E_{nuc}\end{aligned} \tag{2.5}$$

Here we have come to the simplified version of the Schrödinger equation. However, in comparison to the nuclei there are large number of electrons and the $\Psi(\{\vec{x}_i\})$ depends on each coordinates of N electrons. Due to exchange property, Ψ must change sign if two electrons with same spin interchange their position which is a consequence of Pauli exclusion principal. Also, due to correlation property each electron is affected by other electrons in the system. All these make to solve Schrödinger equation difficult for practical life.

2.2 Hartree approximation :

The many body wave function can be written as the product of one electron wave function.

$$\Psi_H(\vec{x}_i) = \phi_1(\vec{x}_1)\phi_2(\vec{x}_2)\phi_3(\vec{x}_3).....\phi_N(\vec{x}_N) \tag{2.6}$$

Here, the index i runs over all electrons under consideration and the wave function $\phi_i(\vec{x}_i)$ represents the single particle states where individual electron is found if this is the realistic approximation. Which we called as *Hartree approximation*. Now, we write the total energy of the system as

$$E_H = \langle\Psi_H|\, H\, |\Psi_H\rangle = \sum_i \langle\phi_i| \Big[-\frac{\hbar^2}{2m_e}\nabla^2 - \sum_{i=1}^{N}\sum_{j>i}^{M} \frac{z_j e^2}{|\vec{r_i} - \vec{R_j}|}\Big] |\phi_i\rangle + \frac{e^2}{2}\sum_{i\neq j} \langle\phi_i|\,\langle\phi_j|\, \frac{1}{|\vec{r} - \vec{r'}|}\, |\phi_i\rangle\, |\phi_j\rangle \tag{2.7}$$

Now by the use of variational principle, the single particle equation can be written as

$$\Big[-\frac{\hbar^2}{2m_e}\nabla^2 - \sum_{i=1}^{N}\sum_{j>i}^{M} \frac{z_j e^2}{|\vec{r_i} - \vec{R_j}|} + e^2 \sum_{i\neq j} \langle\phi_j|\, \frac{1}{|\vec{r} - \vec{r'}|}\, |\phi_i\rangle \Big]\phi_i(\vec{r_i}) = \epsilon_i \phi_i(\vec{r_i}) \tag{2.8}$$

where constant ϵ_i is the Lagrange multiplier. The third term in eq.(2.8) inside the bracket is called the Hartee Potential. Only Coulomb repulsion between electrons are included by Hartee Potential. We can determine each $\phi_i(\vec{r_i})$ if we know $\phi_i(\vec{r_i})$ with i≠j by solving single particle S.E. All these can be done iteratively and schematic representation has been shown below:

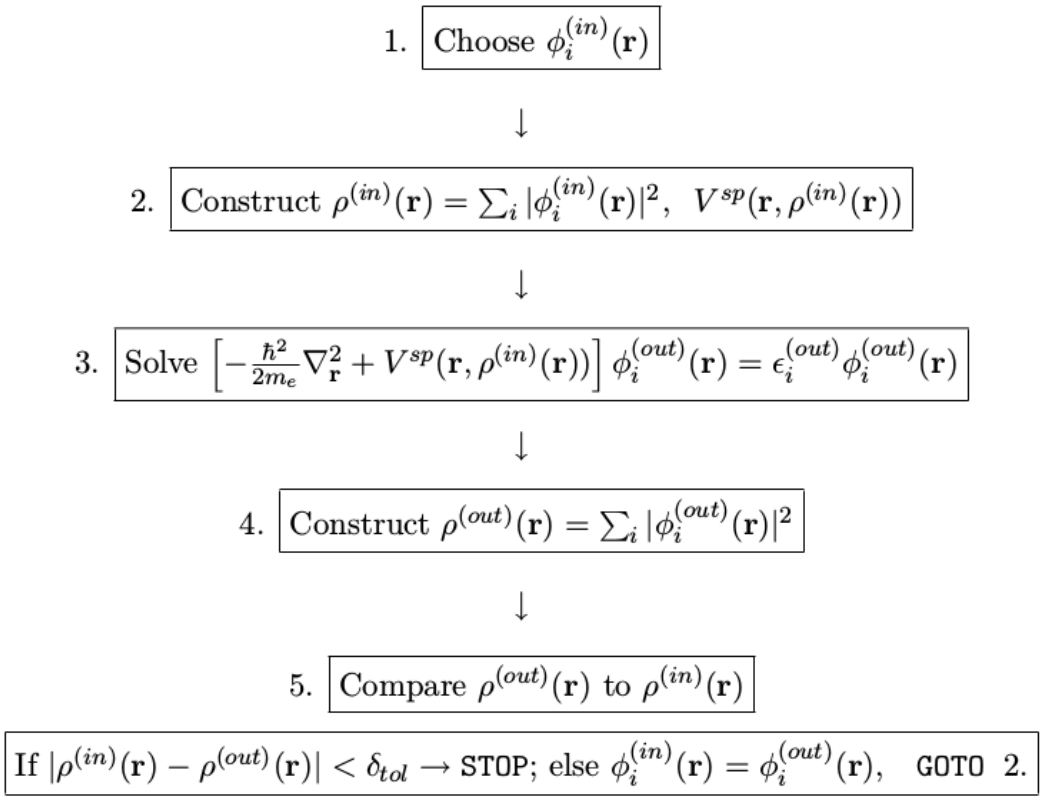

Figure 2.1: Schematic representation of iterative solution of coupled single-particle Hartee equations [16]

2.3 Hartree-Fock approximation :

In Hartree-Fock scheme, we have approximated the N electron wave function by the antisymmetrized product of N one electron wave function $\chi_i(\vec{x}_i)$ in order to incorporate the fermioninc nature of electrons. Slater determinant, Φ_{SD}, given as

$$\Psi \approx \Phi_{SD} = \frac{1}{\sqrt{N!}} \begin{vmatrix} \chi_1(\vec{x}_1) & \chi_2(\vec{x}_1) & \dots & \chi_N(\vec{x}_1) \\ \chi_1(\vec{x}_2) & \chi_2(\vec{x}_2) & \dots & \chi_N(\vec{x}_2) \\ \vdots & \vdots & & \vdots \\ \chi_1(\vec{x}_N) & \chi_2(\vec{x}_N) & \dots & \chi_N(\vec{x}_N) \end{vmatrix}. \tag{2.9}$$

Here, the spin orbitals $\chi_i(\vec{x}_i)$ are composed of spatial orbitals $\phi_i(\vec{r})$ and one of two spin

function $\alpha(s)$ or $\beta(s)$.

$$\chi_i(\vec{x}) = \phi(\vec{r})\sigma(s) \quad ; \sigma = \alpha, \beta \tag{2.10}$$

Spin functions satisfies the property of ortho-normality which is
$\langle\alpha|\alpha\rangle$=$\langle\beta|\beta\rangle$=1
and $\langle\alpha|\beta\rangle$=$\langle\beta|\alpha\rangle$=0.

Also we choose the spin orbitals in such a way that they are orthonormal.

$$\int \chi_i^*(\vec{x})\chi_i(\vec{x})d\vec{x} = \langle\chi_i|\chi_j\rangle = \delta_{ij} \tag{2.11}$$

Where, δ_{ij} is Kronecker delta ($\delta_{ij} = 1$ for $i = j$ and $\delta_{ij} = 0$ for $i \neq j$). Here, the probability of finding the electron with spin σ within the volume element dr is given by $|\chi(\vec{x})|^2$.

Now, the Hartee-Fock energy,E_{HF}.

$$\begin{aligned} E_{HF} &= \langle\Phi_{SD}|\,\hat{\mathrm{H}}\,|\Phi_{SD}\rangle \\ &= \sum_i^N \langle i|\,\hat{\mathrm{h}}\,|i\rangle + \frac{1}{2}\sum_i^N\sum_j^N[\langle ii|jj\rangle - \langle ij|ji\rangle] \end{aligned} \tag{2.12}$$

where,

$$\langle i|\,\hat{\mathrm{h}}\,|i\rangle = \int \chi_i^*(\vec{x}_1)\left\{-\frac{1}{2}\nabla^2 - \sum_j^M \frac{Z_j}{|\vec{r}_1 - \vec{R}_j|}\right\}\chi_i(\vec{x}_1)d\vec{x}_1 \tag{2.13}$$

gives the contribution due to the kinetic energy and electron-nucleus attractive interaction and

$$\langle ii|jj\rangle = \int\int |\chi_i(\vec{x}_1)|^2\frac{1}{r_{12}}|\chi_j(\vec{x}_2)|^2 d\vec{x}_1 d\vec{x}_2 \tag{2.14}$$

are coulomb and exchange integral respectively which represent the interactions between two electrons.

2.4 Thomas-Fermi model :

In 1927 Thomas and Fermi firstly used the electron density to obtain the information about atomic or molecular system. It is a quantum statistical model of electrons. It only takes into account the kinetic energy and treats electron-electron and nuclear-electron interactions in fully classical way. In Thomas-Fermi model, they gave a simple

expression for kinetic energy formula which is based on uniform electron gas and arrive at fictitious model of system of constant density.

$$T_{TF}[\rho(\vec{r})] = \frac{3}{10}(3\pi^2)^{2/3}\int \rho^{5/3}(\vec{r})d\vec{r} \tag{2.15}$$

Above Equation can be combined with nucleus-electron attractive potential and electron-electron repulsive potential. Now the energy functional of Thomas-fermi model is given by,

$$E_{TF}[\rho(\vec{r})] = \frac{3}{10}(3\pi^2)^{2/3}\int \rho^{5/3}(\vec{r})d\vec{r} - Z\int \frac{\rho(\vec{r})}{r}d\vec{r} + \frac{1}{2}\int\int \frac{\rho(\vec{r}_1)\rho(\vec{r}_2)}{r_{12}}d\vec{r}_1 d\vec{r}_2 \tag{2.16}$$

This equation clearly show that energy can be described in terms of electron density $\rho(\vec{r})$.It is an important equation because the information that it provides laid Honenberg and Kohn to think about the conceptual framework of density functional theory. It is the first example of density functional for energy E$[\rho(\vec{r})]$.This equation make us able to map electron density $\rho(\vec{r})$ onto energy E without getting any information about wave function. The assumption of this model is that under a constraint

$$\int \rho(\vec{r})d\vec{r} = N \tag{2.17}$$

there is a connection between the ground state energy and the electron density for which the energy, E_{TF}, is minimum. The energy can be minimized by using the variational principle [17, 18].

2.5 Density Functional Theory

Density functional theory is one of most celebrated and successful quantum mechanical approach to study the many electron problems. In DFT, the density of electrons play a key role instead of many electron wavefunctions. DFT can be applied to a wide variety of the field ie; from organic chemistry to condensed matter physics and can be used to calculate the electronic structure, binding energy of molecules and bands structure [19]. The foundation of *Density Functional Theory*, as it is known today, was laid in 1964 when Hohenberg and Walter Kohn first published their original paper in Physical Review [20] which verified that electron density can be used as basic variable instead of many-body wave function to extract information about material. In 1965, Kohn and Sham , in their paper[21] developed a technique of finding right electron density that involves solving set of single-electron equations. This theory was breakthrough in

understanding material in fundamental way and it opened up a wide avenue for research of complex materials such as carbon nano-tube, protein e.t.c.

2.5.1 Hohenberg-Kohn theorem :

Hohenberg and Kohn gave two theorems in 1964 which are considered as the heart of DFT. They also proved that theorems.
According to the first Hohenberg-Kohn theorem,

"The ground state energy from Schrödinger's equation is unique functional of the electron density $\rho(\vec{r})$[22]."
In other words, the density $\rho(\vec{r})$ is uniquely defined for given external potential $V(\vec{r})$ for electrons. we can prove this as follows.

Let us consider $V(\vec{r})$ and $V'(\vec{r})$ are two non-trivially different potentials ($i.e$ not just different by mere constant). We also assume that the two different potential $V(\vec{r})$ and $V'(\vec{r})$ give rise to the same density $\rho(\vec{r})$.
Let E and E$'$ be the total energies. Since the two external potetials are different so they must have two different wave function Ψ and Ψ' for the systems with two different hamiltonian H and H$'$ respectively. Here, hamiltonian H is defined with potential $V(\vec{r})$ and H$'$ is defined with potential $V'(\vec{r})$.

$$E = \langle \Psi | H | \Psi \rangle \tag{2.18}$$

$$E' = \langle \Psi' | H' | \Psi' \rangle \tag{2.19}$$

Now by using the variational principle, we can write,

$$\begin{aligned} E < \langle \Psi^{'} | H | \Psi^{'} \rangle &= \langle \Psi^{'} | H^{'} + V - V^{'} | \Psi^{'} \rangle \\ &= \langle \Psi^{'} | H^{'} | \Psi^{'} \rangle + \langle \Psi^{'} | (V - V^{'}) | \Psi^{'} \rangle \\ &= E^{'} + \langle \Psi^{'} | (V - V^{'}) | \Psi^{'} \rangle \end{aligned} \tag{2.20}$$

Here, inequality is due to fact that two potentials are completely different in non-trivial way. Similarly we can show that

$$E^{'} < E - \langle \Psi | (V - V^{'}) | \Psi \rangle \tag{2.21}$$

Adding equation 2.18 and equation 2.19, we get

$$(E + E^{'}) < (E + E^{'}) + \langle \Psi^{'} | (V - V^{'}) | \Psi^{'} \rangle - \langle \Psi | (V - V^{'}) | \Psi \rangle \tag{2.22}$$

Here, last two terms gives

$$\langle \Psi^{'} | \left(V - V^{'}\right) | \Psi^{'} \rangle - \langle \Psi | \left(V - V^{'}\right) | \Psi \rangle = \int \rho^{'}(\vec{r})[V(\vec{r}) - V^{'}(\vec{r})]d\vec{r} - \int \rho(\vec{r})[V(\vec{r}) - V^{'}(\vec{r})]d\vec{r}$$
$$= 0, \tag{2.23}$$

because of our initial assumption that densities $\rho(\vec{r})$ and $\rho^{'}(\vec{r})$ are same. This leads to contradictory condition

$$(E + E^{'}) < (E + E^{'}) \tag{2.24}$$

Here the equation (2.24) is not possible, which implies that our initial assumption must be wrong. Hence, the two external potential can not yield the same ground state electron density. From this, we conclude that there must exist one-to-one correspondence between external potential V($\vec{r}$) and electron density $\rho(\vec{r})$. Since the wave function is determined by the external potential, and therefore wave function must also be unique functional of electron density. If the hamiltonian is the sum of kinetic energy term (T) and electron-electron interaction term (U) other than V i.e $H = T + U$ then the universal functional of density must exist as

$$F[\rho(\vec{r})] = \langle \Psi | \left(T + U\right) | \Psi \rangle \tag{2.25}$$

Since the kinetic energy (T) and electron-electron interactions (U) terms are common to all solids. Thus this functional only depends on electron density which is uniquely determined by external potential V. the external potential depend upon the what type of system we are dealing with *i.e* which differs from system to system. Thus, the total energy of system can be written as functional of density as

$$E[\rho(\vec{r})] = \langle \Psi | H | \Psi \rangle = F[\rho(\vec{r})] + \int V(\vec{r})\rho(\vec{r})d\vec{r} \tag{2.26}$$

Although, first HK theorem proves that the external potential is the unique functional of electron density. However, it can not say anything about which is the actual electron density. A very important property of the functional is given by the 2^{nd} HK theorem. It states that

"The true electron density is that which minimizes the energy of the overall functional corresponding to the full solution of the Schrödinger equation[22]."
if we know the true form of the functional, by using the variational principle, we can

vary the electron density until we get the minimum energy from the functional But however, we are unaware of the true form of functional , thus making this idea of no practical use.

2.5.2 Kohn-Sham approach :

In 1965, Kohn and Sham [23] give an approach to deal with unknown functional which we already discussed in our previous section. Kohn and Sham gives the contribution for the costruction of more practical set of equation by using equation. Kohn-Sham approach to the problem considers the fictitious system containing non- interacting electrons where total wave function of the system is given by Slater determinant in accordance with the Hartree-Fock approximation.
In HK theorem the ground state energy can be written as

$$E_0[\rho] = \min_{\rho \to N} F[\rho(\vec{r})] + \int \rho(\vec{r}) V(\vec{r})\, d\vec{r}. \tag{2.27}$$

Here, F$[\rho(\vec{r})]$ is the universal functional. This function contains kinetic energy, classical coulomb interaction and non-classical portion due to self-interaction correction, exchange and correlation effects.

$$F[\rho(\vec{r})] = T[\rho(\vec{r})] + J[\rho(\vec{r})] + E_{ncl}[\rho(\vec{r})]. \tag{2.28}$$

Among all these three energy term, we know only J$[\rho(\vec{r})]$, while we don't know the explicit form of other two terms.
To understand the Kohn-Sham approach, we first briefly review Hartee-Fock method. The kinetic energy can be written as

$$T_{HF} = -\frac{1}{2} \sum_{i}^{N} \langle \chi_i | \nabla^2 | \chi_i \rangle . \tag{2.29}$$

Here, we choose the spin orbitals χ_i in order to attain the minimum value of the energy E_{HF} under the constrains that χ_i remains orthogonal.

$$E_{HF} = \min_{\Phi_{SD} \to N} \langle \Phi_{SD} | \hat{T} + \hat{V} + \hat{V}_{ee} | \Phi_{SD} \rangle \tag{2.30}$$

Now, we introduce the local potential $V_s(\vec{r})$ to interpret a non-interacting reference system with Hamiltonian

$$H_S = -\frac{1}{2} \sum_{i}^{N} \nabla_i^2 + \sum_{i}^{N} V_S(\vec{r}_i). \tag{2.31}$$

We can easily see that there is no any electron-electron interaction terms in such Hamiltonian, so it is able to describe non-interacting system. The corresponding ground state wave function is given by the slater determinant as

$$\Theta_S = \frac{1}{\sqrt{N!}} \begin{vmatrix} \phi_1(\vec{x}_1) & \phi_2(\vec{x}_1) & \dots & \phi_N(\vec{x}_1) \\ \phi_1(\vec{x}_2) & \phi_2(\vec{x}_2) & \dots & \phi_N(\vec{x}_2) \\ \vdots & \vdots & & \vdots \\ \phi_1(\vec{x}_N) & \phi_2(\vec{x}_N) & \dots & \phi_N(\vec{x}_N) \end{vmatrix}. \tag{2.32}$$

We solve the equation

$$\hat{\mathrm{f}}^{KS}\phi_i = \epsilon_i\phi_i \tag{2.33}$$

to obtain spin orbitals where, $\hat{\mathrm{f}}^{KS}$ can be recognized as one-electron Kohn-Sham operators and is defined as

$$\hat{\mathrm{f}}^{KS} = -\frac{1}{2}\nabla^2 - V_S(\vec{r}) \tag{2.34}$$

Here, spin orbitals ϕ_i are called Kohn-Sham orbitals. Now, we choose V_S in such a way that the density of non-interacting fermions in fictitious system is exactly equal to ground state density of real system of interacting electrons.

$$\rho_S(\vec{r}) = \sum_i^N \sum_s |\phi_i(\vec{r}, s)|^2 = \rho_o(\vec{r}) \tag{2.35}$$

2.5.3 Kohn-Sham equations :

The brilliance of Kohn and Sham is in realizing that if it is not possible to calculate kinetic energy accurately through explicit functional then one should calculate as much as one can of the true kinetic energy exactly and deal remainder in approximately. To obtain the exact kinetic energy of the non-interacting reference system with same density as that of real interacting system, Kohn and Sham suggested to use equation(2.30) as

$$T_S = -\frac{1}{2}\sum_i^N \langle\phi_i| \nabla^2 |\phi_i\rangle \tag{2.36}$$

Obviously, the kinetic energy of non-interacting reference system is not equal to true kinetic energy of real interacting system. To account this. Kohn and Sham introduced the following separation of functional $\mathrm{F}[\rho]$

$$F[\rho(\vec{r})] = T_S[\rho(\vec{r})] + J[\rho(\vec{r})] + E_{XC}[\rho(\vec{r})] \tag{2.37}$$

where E_{XC} is called exchange-correlation energy defined as

$$E_{XC}[\rho] \equiv (T[\rho] - T_S[\rho]) + (E_{ee}[\rho] - J[\rho]) = T_c[\rho] + E_{ncl}[\rho] \tag{2.38}$$

The remainder part of true kinetic energy,T_C, which is not covered by T_S, is added to the non-classical electrostatic contributions. Thus, E_{XC} not only contains the non-classical effects of exchange and correlation, self-interaction correction, which contributes to the potential energy of the system, but also the portion of kinetic energy that cannot be calculated exactly. Expression for energy of non-interacting reference system is composed of two part: kinetic energy and energy due to interaction with external potential. From HK theorem, we learned that the total energy must be the functional of density. Similarly, the interaction with external potential is an explicit functional of density, ρ. Hence, T_S must also be the functional of density. But it is necessary to note that density does not appear in expression for T_S explicitly: KS orbital appear in equation(2.37) not the density.

To define V_S such that it gives the Slater determinant which is characterized by the same density as that of our real system, we write the expression for energy of real interacting system as

$$\begin{aligned} E[\rho(\vec{r})] &= T_S[\rho] + J[\rho] + E_{XC}[\rho] + E_{Ne}[\rho] \\ &= T_S[\rho] + \frac{1}{2}\iint \frac{\rho(\vec{r})\rho(\vec{r})}{r_{12}}\, d\vec{r}_1\, d\vec{r}_2 + E_{XC}[\rho] + \int V_{Ne}\rho(\vec{r})\, d\vec{r} \\ &= -\frac{1}{2}\sum_i^N \langle\phi_i|\,\nabla^2\,|\phi_i\rangle + \frac{1}{2}\sum_i^N\sum_j^N \iint |\phi_i(\vec{r}_1)|^2 \frac{1}{r_{12}} |\phi_j(\vec{r}_2)|^2\, d\vec{r}_1\, d\vec{r}_2 \\ &+ E_{XC}[\rho(\vec{r})] - \sum_i^N \int \sum_A^M \frac{Z_A}{r_{1A}} |\phi_i(\vec{r}_i)|^2\, d\vec{r}_1 \end{aligned} \tag{2.39}$$

Now we apply variational principle to minimize energy expression under usual constraint of $\langle\phi_i|\,|\phi_j\rangle = \delta_{ij}$. The resulting equations are

$$\begin{aligned} &\left(-\frac{1}{2}\nabla^2 + \left[\int \frac{\rho(\vec{r}_2)}{r_{12}}\, d\vec{r}_2 + V_{XC}(\vec{r}_1) - \sum_A^M \frac{Z_A}{r_{1A}} \right] \right) \phi_i \\ &= \left(-\frac{1}{2}\,\nabla^2 + V_{eff}(\vec{r}_1) \right) \phi_i = \epsilon_i \phi_i \end{aligned} \tag{2.40}$$

Compairing this equation with equation(2.34), we find that the term V_{eff} is identical to V_S. Therefore, we have

$$V_S(\vec{r}) \equiv V_{eff}(\vec{r}) = \int \frac{\rho(\vec{r}_2)}{r_{12}}\, d\vec{r}_2 + V_{XC}(\vec{r}_1) - \sum_A^M \frac{Z_A}{r_{1A}}. \tag{2.41}$$

Here, V_{XC} is potential due to the exchange-correlation energy E_{XC} and is simply defined as functional derivative of E_{XC} with respect to ρ, i. e.,

$$V_{XC} \equiv \frac{\delta E_{XC}}{\delta \rho} \tag{2.42}$$

Knowing all the contribution in equation(2.41), we can have V_S which can be used in one-particle equations to find KS orbitals and hence ground state density can be determined using equation(2.35) and the ground state energy using equation(2.39). But it is to be noted that V_S already depends on density and thus on the KS orbitals. There fore one-particle KS equations must be solved iteratively. Algorithm for solving KS equation can be illustrated as shown in figure below.

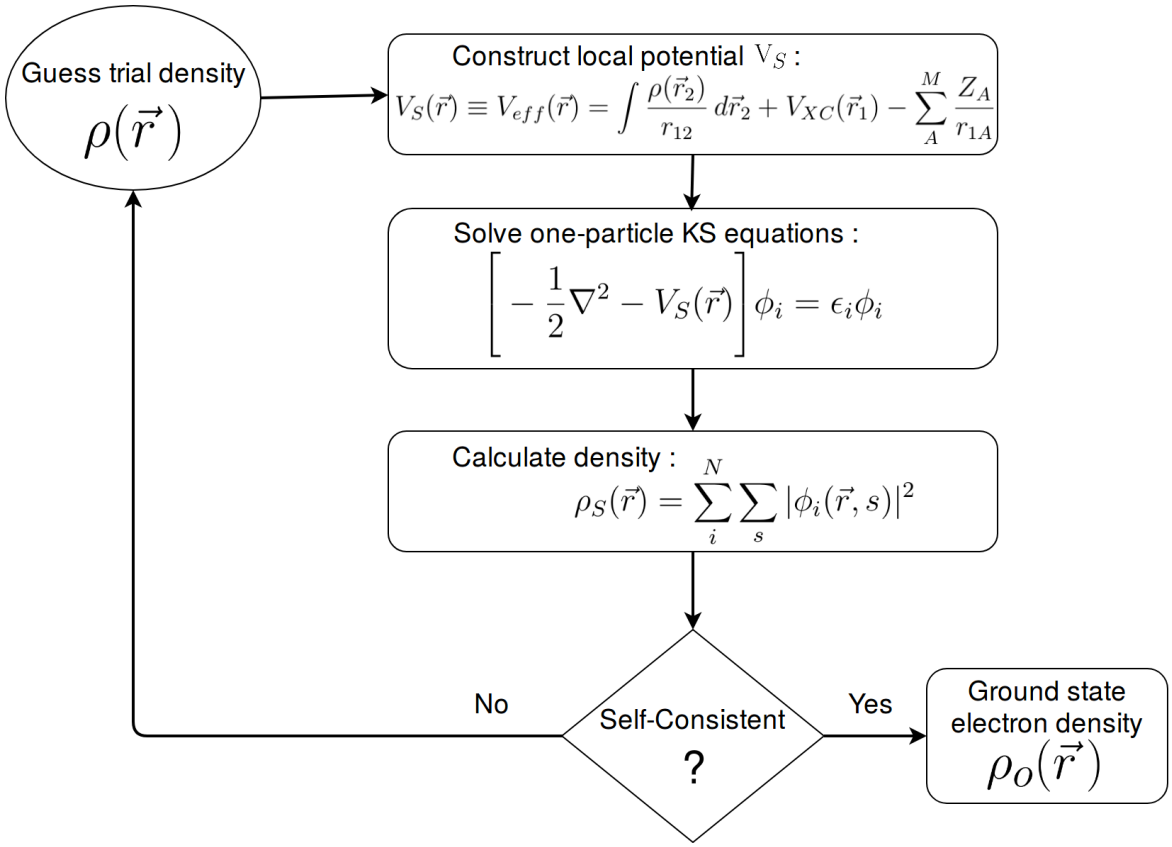

Figure 2.2: Schematic diagram illustrating algorithm to solve KS equations [24].

At first we take any trial density $\rho(\vec{r})$. By using this trial density we can construct local potential $V_s(\vec{r})$ which we can also say an effective potential $V_{eff}(\vec{r})$. After constructing this potential we can now able to solve one particle Kohn-Sham equation. The Kohn-Sham equation provides the solution for Kohn-Sham orbital ϕ_i. Now, we can calculate the density of non-interacting fermions in fictitious system. If this is self consistent then this density is equal to the ground state density and we stop our calculations. However, if the self consistency is not achieved then we follow the same procedure until we get the self consistency.

2.5.4 Exchange correlation functional :

We can apply the Kohn-Sham formalism if we know exactly the explicit form of E_{XC} ie; exchange-correlation functional. We have to choose a better functional for our system. There are many approximation to explicit form of exchange-correlation functional. Among them, we use mostly the Local density approximation (LDA) and generalized gradient approximation (GGA).

Local Density Approximation(LDA):

It is the simplest and good approximation. The local density approximation is exact for a homogeneous interacting system where the electron density is constant [25]. The LDA is

$$E_{xc}^{\mathrm{LDA}}[\rho(\mathbf{r})] = \int \rho(\mathbf{r}) e_{xc}(\rho(\mathbf{r}))\, d^3r$$

Local Spin Density Approximation(LSDA):

In case of spin polarized system, it is better to use local spin density approximation for DFT calculation. it gives the more accurate results for those system [25]. The LSD approximation is

$$E_{xc}^{\mathrm{LSD}}[\rho_\downarrow, \rho_\uparrow] = \int \rho(\mathbf{r}) e_{xc}(\rho_\downarrow(\mathbf{r}), \rho_\uparrow(\mathbf{r}))\, d^3r$$

where, e_{xc} is the known exchange-correlation energy per particle for an electron gas of uniform spin densities $\rho_\downarrow$ and $\rho_\uparrow$.

Generalised Gradient Approximation(GGA):

In case of a system where electron density is inhomogeneous, GGA is the best approximation [26]. The GGA is

$$E_{xc}^{\mathrm{GGA}}[\rho_\downarrow, \rho_\uparrow] = \int f(\rho_\downarrow, \rho_\uparrow, \nabla\rho_\downarrow, \nabla\rho_\uparrow)\, d^3r$$

2.6 Density functional theory with Vander Waals (vdW) correction

Up to now, we discussed about DFT and treated DFT as a exact theory and referred it as tool of giving accurate calculations. But however, there is some approximation

that we need to make to treat our calculations in practical scheme. In practice, there is an interaction between the electrons and we ought to incorporate this interaction. Since exchange correlation functional can't describe the long range electron correlations. However, such long range correlations are responsible for the vdW interaction. in vdW interaction, there is a term $\frac{-1}{r^6}$. This term arises from the instantaneous dipole induced dipole contribution. This term signifies the decay of the interaction energy with the inter atomic separation r. To incorporate the missing long range interaction we simply add the additional energy term with the energy obtained from DFT calculations as

$$E_{Tot} = E_{DFT} + E_{dis} \tag{2.43}$$

Here, E_{Tot} is the total energy for DFT with exchange and correlation functional and E_{dis} is the contribution from the dispersive interaction and it is given by

$$E_{dis} = \sum_{i,j} \frac{c_6^{i,j}}{r_{i,j}^6} \tag{2.44}$$

Here, $c^{i,j}$ is the dispersive coefficients for the elemental pairs. However, this term only includes the leading term and disregard mostly the many body dispersion and for very large separation of atoms this term diverges. However, such a divergence can be removed by use of DFT-D2 scheme [27, 28].

2.6.1 Pseudopotential

Our computational software uses the technique that comes from the idea of pseudopotential. The concept of pseudopotential was first introduced by Fermi to study high-lying atomic states which on later, Hellman proposed that pseudopotential can be used for calculating the energy levels of the alkali metals. In this technique, we replace the actual potential energy and filled shells in the core region by an effective potential energy such that the resultant wave function outside the core will be same as given by the actual ion cores called psueudopotential. Use of pseudopotential makes calculation easy and reduces computational cost without significant change in calculated results

Chapter 3

Details of Simulation

3.1 Implementation of DFT

Our present work is computational based on the density functional theory (DFT). In this work, we have implemented pseudo-potential plane wave based method using Quantum ESPRESSO package.

3.1.1 The Quantum ESPRESSO code

Quantum-ESPRESSO is an abbreviation for Quantum opEn-Source Package for Research in Electronic Structure, Simulation, and Optimization. We use computational method with Quantum ESPRESSO as a required simulation package. It is an integrated suite of computer codes for electronic-structure calculations and materials modeling, based on density-functional theory, plane waves, and pseudopotentials [29]. It is based on density-functional theory first-principles calculations which is performed by using plane waves basis set, and pseudopotentials. Quantum-ESPRESSO can conduct the ground state calculations such as Self-consistent total energies, forces, stresses, Kohn-Sham orbitals and exchange-correlation functionals due to Local Density Approximations and Generalized Gradient Approximations [30]. The Quantum ESPRESSO package have following as a main components [31].

PWscf

PWscf [**P**lane-**W**ave **s**elf-**c**onsistent **f**ield] is one of core component of Quantum ESPRESSO distribution. Pwscf performs different electronic-structure calculation within Density Functional Theory, using plane-wave basis set and pseudo-potential to represent electron-ion interactions. In particular, it can calculate ground state energy, one-electron KS orbitals, atomic forces and stress, molecular dynamics, structural optimization e.t.c. It can use the LDA, GGA including the spin polarization. It uses the norm conserving pseudo potential, ultrasoft pseudo potential and in present days the projector augmented wave method. It helps to perform self consistent calculations, structural relaxation, electronic structure calculation and variable cell molecular dynamics. We have taken an account of ion dynamics by using Broyden-Fletcher-Goldfarb-Shanno (BFGS) for structural optimizations. An input file of QE consists of following as main parameters:

- **calculation**: We have to specify here that we are going to perform Calculations like scf, bands, relax, vc-relax, nscf, DOS , PDOS can be performed and if we perform scf calculation, we write calcualtion='scf' in our input file and similarly for others.

- **ibrav**: For fourteen different Bravias lattice, we can assign the ibrav different value from 1 to 14. Hence ibrav specifies the type of bravis latttice we are simulating. We can also generate the desired crystal structure using ibrav = 0.Here, for hexagonal boron nitride we have taken ibrav=4.

- **celldim(i)**: i = 1,2,3 specifies the lattice parameters of the crystal and are usually given in atomic units where as i = 4, 5, 6, are the cosines of the angles between each pair of lattice parameters. In our case celldm(1) = a = celldm(2) and celldm(3)= c/a where a, b and c are lattice vectors along X,Y and Z direction.

- **celldim(3)**= c/a where a, b and c are lattice vectors along X,Y and Z direction respectively

- **ecutwfc**: It is the kinetic energy cutoff, which limits the amount of plane wave basis that is used for the ground state calculations. It is expressed in unit of the energy Rydbergs (Ry) or eV.

- **nat**: It represents the number of atoms in the system under study.

- **ntyp**: It gives the number of types of atoms used in simulating unit.

- **ATOMIC SPECIES**:It signifies the symbols of atoms, their corresponding masses (in a.m.u.) and the name of the files containing pseudo-potentials (PPs). For instance: for boron atom B 10.8110 B.pbe-n-rrkjus psl.0.1.UPF.

- **ATOMIC POSITIONS**: It represents the co-ordinates of atoms in our unit cell. It can be in Angstrom, Bohrs etc.

- **K-POINTS**: It denotes the number of sampling points in the reciprocal space in which actual self-consistent minimization of energy will be performed. Higher the value of k-points taken better is the precision. K-points are taken from the convergence test.The k-points at which the Brillouin zone is to be sampled during a self consistent calculation to find the electronic ground state.

PostProc

It contains a large number of codes and has become a boon for analyzing the data files generated by PWscf calculations. These codes can be used for band structure calculations, DOS, Projected density of states calculations. Among them, the most used codes are:

- **bands.x**: This code has been used to extract the data files from PWscf calculations and records its eigen value for different k-points with corresponding k-points which is used for further calculations.

- **plotband.x**: **bands.x** generates many different files that has been utilized by **plotband.x** to plot the band structure.

- **dos.x**: This code is used to calculate the electronic density of states.

- **projwfc.x**: This code is utilized to calculate the projection of wave functions over atomic orbitals which performs population analysis and calculates the projected density of states(PDOS). PDOS gives us the contribution to electronic density of states by different atomic orbitals like s, p, d and so on.

We have visualized our crystal structure by using XCrysDen and all graphs have been plotted with the use of Xmgrace.

3.1.2 XCrySDen

It is very useful to visualize our molecular and the crystalline structure. It also possess some important tools that helps to visualize the system in a reciprocal space. For ex;

the selection of k-paths in Brillouin zone for the band structure plots and also used in visualization of a fermi surfaces [32].

3.2 VESTA

VESTA is a 3D visualization software and VESTA stands for Visualization for Electronics and STructural Analysis. It is use to observe teh structural model, volumetric data, electron/nuclear densities and crystal morphologies. Here, we have used the VESTA version 3.4.8.

3.2.1 Xmgrace

It is a 2D plotting tool and stands for "GRaphing, Advanced Computation and Exploration of data. It is used to modify plots, set all kind of plot parameters, change the appearance of your graph, and to save the figure in the format of your interest. It can be used to plot any sets of data from file with multiple columns (bolck data) and load data from different files in a single plot [33].

3.3 Computational details

We have studied the structural stability, electronic and magnetic properties of pure and single vacant hBN sheet. These calculations have been performed by using Density functional theory (DFT) with van der Waals (vdW) interactions in DFT-D2 approach by utilizing Quantum espresso code [30]. We have accounted the electronic exchange and correlation effect in our system by utilizing the generalized gradient approximation (GGA) developed by Perdew, Burke and Ernzerhof (PBE) [26].

After performing relax calculations of our system, we have performed self consistent calculations by sampling brillouin zone of hexagonal boron nitride in K-space using Monkhorst-Pack scheme [34] with appropriate number of mesh of K-points that has been determined by the convergence test.

3.3.1 Construction of Hexagonal Boron Nitride Monolayer

Hexagonal Boron Nitride has a honeycomb structure, where equal number of Boron and Nitrogen atoms are alternatively arranged. There is covalent bond between Boron and

Nitrogen atoms, whereas the different layers of Boron Nitride are held by weak van der Waal force. The bond angle between Boron and Nitrogen is 120^0. Since, we are working on monolayer of h-BN, we only take account of covalent bond and neglect the van der waal force.

For our study, we have to work on unit cell which contains one Boron and one Nitrogen covalently bonded together. The atomic positions are calculated using the simple geometry of the crystal.The lattice parameter c was taken 20 Å for we studied two dimensional h-BN. In the input file of Quantum ESPRESSO we set ibrav=4, celldm(1)= 4.74, celldm(3)= 7.97 expressed in Bohrs which is called alat and celldm(3) c is expressed in units of celldm(1)) and calculated atomic positions (in alat) in the primitive unit cell geometrically.

In order to obtain the optimized structure of h-BN monolayer, we have to optimize the different parameters. So, the next important step is to optimize the value of kinetic energy cutoff for the plane wave (ecutwfc), lattice parameter and the k-points applying convergence tests.

3.3.2 Convergence Tests

We have performed scf calculations to determine the three basic parameters as mentioned above by testing the convergence of total energy with these parameters individually.

Kinetic energy cutoff (ecutwfc)

Quantum Espresso implements plane wave self consistent field (PWscf) code to expand electronic wave function in terms of infinite basis function and are called plane waves. Bloch theorem states that,

$$\psi_{\mathbf{k}}(\mathbf{r}) = \exp(i\mathbf{k}.\mathbf{r})u_{\mathbf{k}}(\mathbf{r}) \tag{3.1}$$

where

$$u_{\mathbf{k}}(\mathbf{r} = \sum_{G} C_G \exp i(\mathbf{k} + \mathbf{G}).\mathbf{r} \tag{3.2}$$

Here, $\psi_{\mathbf{K}}(\mathbf{r})$ represents the electronic wave function and $u_{\mathbf{k}}(\mathbf{r})$ be the periodic wave function in lattice. In above equation, $\mathbf{G}$ runs over all the reciprocal lattice vectors and

the coefficient C_G is the expansion coefficient. Here the term infinite basis is only an ideal case and practically it is not possible so we have to truncate it after obtaining certain value of basis function. We can define the kinetic energy cut off as the value of kinetic energy that corresponds to the cut off value of the basis function. We focus on the situation whether the measured difference in energy between two consecutive iteration is within our converging limit or not and determine a suitable truncating limit. We can truncate eq.(3.2) by using the following condition:

$$\frac{|k+G|^2}{2m} \leq E_{cut} \tag{3.3}$$

The value of the kinetic energy (in Rydberg) corresponding to the cut off value is the kinetic energy cut-off(E cut). Using the arbitrary k-point mesh ($18 \times 18 \times 1$) and the experimental values of atomic positions and lattice parameters we executed the scf calculations for different values of ecutwfc (25, 30, 35, 40, 45, 50, 55, 60, 65, 70)Ry, with executable pw.x. The plot of total energy versus kinetic energy cut off using xmgrace is obtained as in figure below.

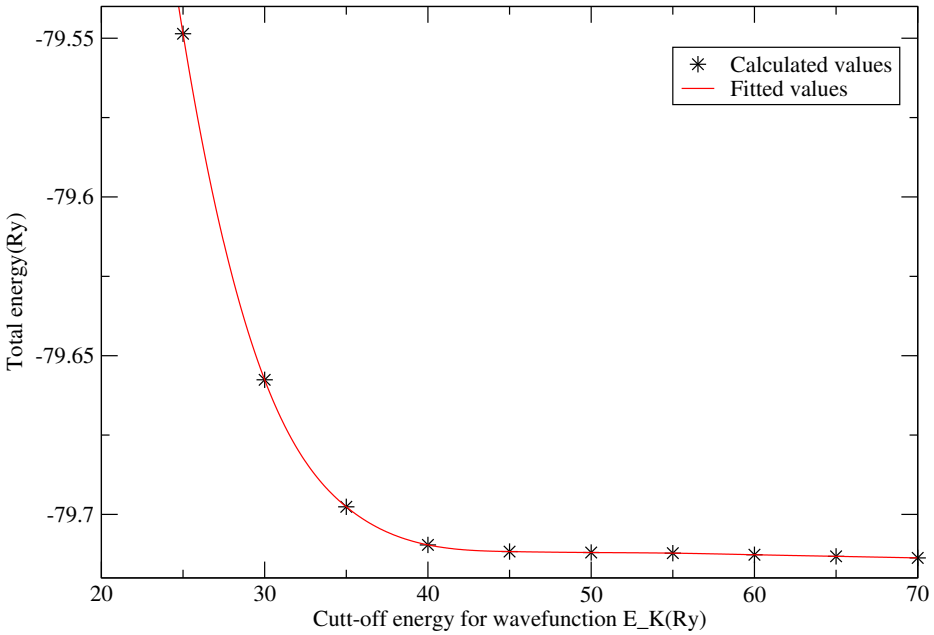

Figure 3.1: Total energy of h-BN primitive cell vs Kinetic energy cut-off

Convergence with respect to K-points

It is the number of the points in the reciprocal space that the program is supposed to sample i.e. the points in which the actual self-consistent minimization of the energy will

be performed. Using the ecutwfc = 45 Ry and the experimental value from published works we set the celldm(1)=4.74 and celldim(3)=7.97 and ran the scf calculations for different values of k-points (3, 6, 9, 12, 15, 18, 21, 24, 27) along the k_x and k_y direction and single k-point along the k_z direction. The plot of total energy convergence with respect to different k-points grid size is shown in figure . The optimal size of k-point mesh was chosen to be $18 \times 18 \times 1$ as energy convergence around this size was found to be with in our total energy convergence threshold for scf calculation.

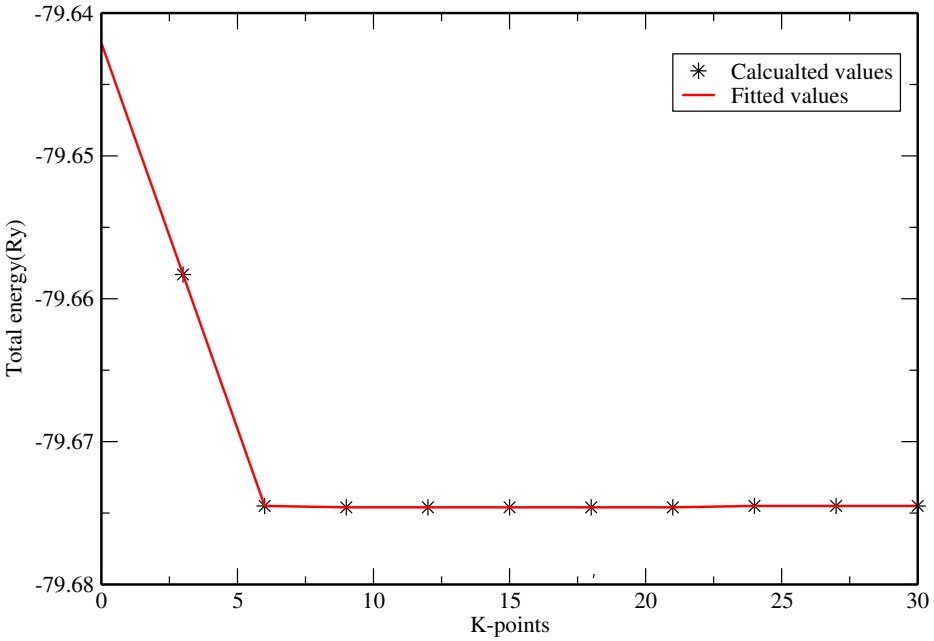

Figure 3.2: Total energy vs K-points

Convergence with respect to lattice parameter

Here, we optimize the value of lattice parameter . In order to fix the lattice parameter a we set interlayer spacing along z-direction to be 20 Å and hence run scf calculation for a_0 = (4.64, 4.66, 4.68, 4.70, 4.72,4.73, 4.74, 4.75, 4.76,4.78, 4.80, 4.82, 4.84) Å. Thus obtained energies are plotted against lattice parameter a_0 as in figure. The figure shows parabolic nature with it's vertex at 4.74 Å along X-axis that is the point of minimum energy.

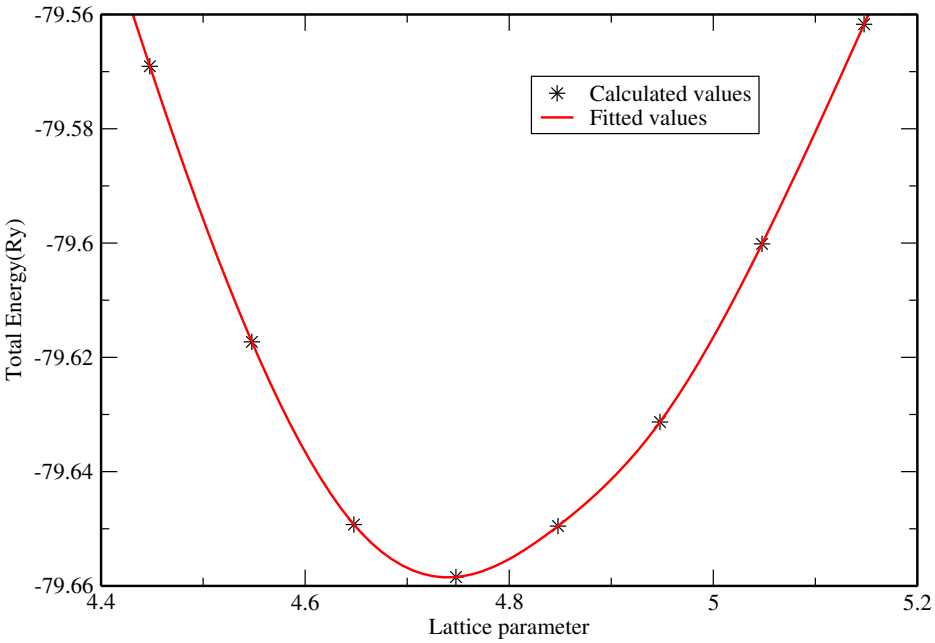

Figure 3.3: Total energy vs lattice parameter (a_0)

Chapter 4

Results & Discussion

4.1 General Consideration

In this section, we present our outcomes along with their proper analysis. We have implemented spin polarized density functional theory to perform our all calculations. Before entering to main calculations, we have performed convergence tests for ecutwfc, lattice parameter 'a' and k-points in order to obtain the optimized and the most stable structure for our calculations. After getting an optimized system for our main calculation we proceed to study the stability of pure hBN sheet, single vacant hBN sheet in which we have studied different properties with nitrogen vacancy and boron vacancy. We have also studied the structural, electronic and the magnetic properties of the respective system by studying the structural parameters, band structures, and density of states for each systems.

4.2 Results and Discussion

By implementing density functional theory (DFT), We have presented our results in order to obtain the following :

- Structural geometry and the stability of pristine hBN sheeet
- Structural geometry and the stability of single Nitrogen and single Boron vacant hBN sheet
- band structure of pure and single vacant h-BN sheet.

- Density of states (DOS) calculation of pristine hBN sheet, single Nitrogen vacant and single Boron vacant hBN sheet
- PDOS of pristine and single vacant h-BN sheet

4.2.1 Structural Properties of pure hexagonal boron nitride (hBN)

We already discussed about the convergence and optimization tests that we had performed. Taking those optimized values of ecutwfc, k-points and the lattice parameter we defined our system in the PWscf input file. Taking the help of XCrySDen we first obtained the primitive cell structure and then that of the 4×4 supercell, using this input file. The both primitive cell and supercell were allowed to relax using BFGS quasi-newton algorithm for structural relaxation.

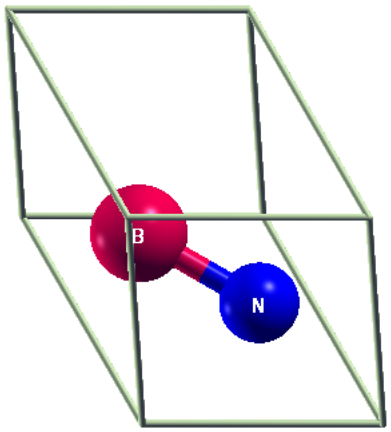

Figure 4.1: Optimized primitive cell

We found very change in the atomic position after relaxation and thus very small variations in bond lengths and bond angles are observed as shown in table (4.1). We can see in figure (4.1), B and N atoms lie symmetrically along the diagonal in a plane at some

height in the primitive cell. This height can be given an arbitrary value with in the cell as h-BN is layered material with both B and N lying nearly at same height from basal plane.

Table 4.1: Optimized structural parameters of the relaxed system in study

Primitive cell (2 atoms)	Lattice parameter	a=b=2.51 Å, c=20.02 Å
	B-N bond length	1.45 Å
4x4 Supercell (32 atoms)	Unit cell size	a=b= 10.03 Å, c=20 Å
	B-N bond lengths	1.44 Å,1.44 Å, 1.44 Å
	N-B-N bond angles	120^0

The relaxed primitive cell structure is shown in the figure above and the structural parameters are tabulated in the table. The experimental values of B-N bond lengths and N-B-N bond angles are respectively 1.440 Å and 120^0.

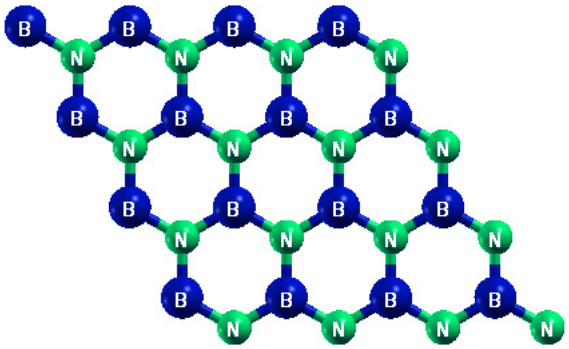

Figure 4.2: (4×4) Supercell of monolayer h-BN contains 32 atoms.

As already stated in table about the value of lattice parameter along z-axis (c) is equal to 20Å which is nearly three times as large as that of bulk h-BN (6.66 Å). There is a

very small discrepancy in one of the bond angle which we believe is agreeable within our convergence threshold of total energy and force on each atom. After obtaining the desired structure and geometry of pure h-BN we used copies of the input files, we create a single vacancy by removing one Boron and one Nitrogen separately so that atoms in a unit cell are decreased by one for the vacant system. Now the system is a unit cell with 31 atom basis with 2 atomic species. Thus, we obtained two different inputs for V_B and V_N systems with which we ran the relax calculation by using executable pw.x. The relaxed coordinates were used to create a input file for scf calculation.

Table 4.2: Structural parameters of the h-BN sheet with Boron Vacancy(V_B)

Structural detail of 4x4 h-BN sheet with V_B	
N-B-N bond angles	123.94^0, 123.94^0, 123.94^0
Nearest neighbor B-N-B bond angles	118.23 ^{0},118.23 ^{0}, 118.23 ^{0}
Nearest neighbor B-N bond length towards V_B	1.41 Å

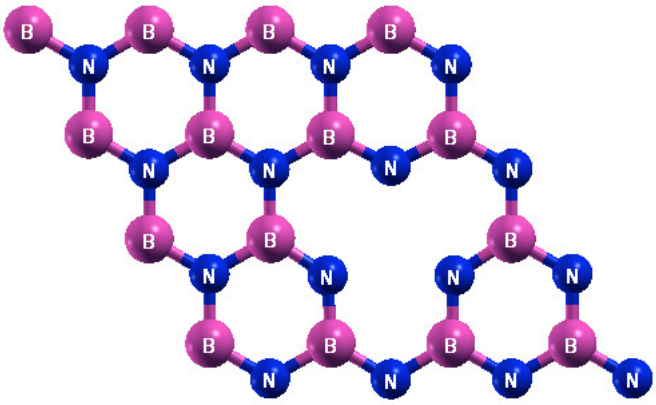

Figure 4.3: Single Boron vacant site of h-BN after relaxation.

Table 4.3: Structural parameters of the h-BN with Nitrogen Vacancy(V_N)

Structural detail of 4x4 h-BN sheet with V_N	
B-N-B bond angles	119.71^0, 119.71^0, 119.71^0
Nearest neighbor N-B-N bond angles	115.72 ^{0},115.72 ^{0}, 115.72 ^{0}
Nearest neighbor B-N bond length towards V_N	1.46 Å

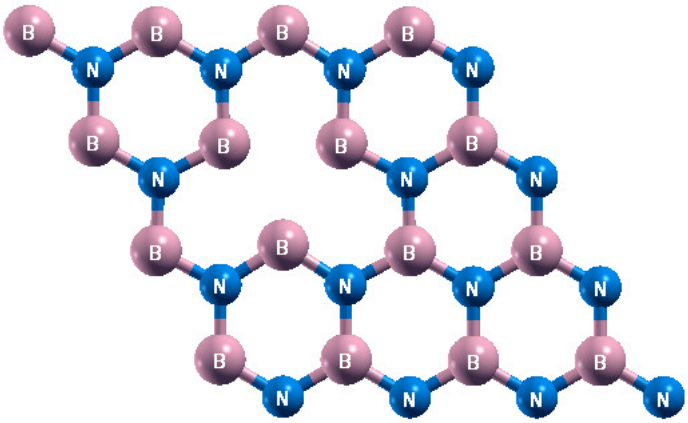

Figure 4.4: Single Nitrogen vacant site of h-BN after relaxation.

As we create the single vacancy on the pure h-BN by removing Boron and Nitrogen, several changes has been observed. The nearest neighbor B-N bond lengths and bond angles are altered. The B-N bond is covalent yet slightly ionic. The different structural characteristics of single vacant hBN can be seen from the above tables (4.2) and (4.3).

From above table it is seen that for both Boron and nitrogen vacancy, triangular shaped structure has been seen. Also the bond angles N-B-N and B-N-B towards the vacant side are slightly different which is shown in the above table. We also discussed for nearest neighbor bond lengths and bond angles around the site to study the structural modification in overall sheet. We found that nearest neighbor bond angles are found

to be 118.23^0 in V_B. But for V_N nearest neighbor bond angle is about 115.72^0. In above case The B-N bond length in non-defective region is found to be 1.43 Å which is comparable to experimental value 1.44 Å with error of 0.1Å.[8].

Boron and Nitrogen are experimentally distinguished first time by means of aberration corrected high-resolution transmission electron microscopy (HRTEM) with exit wave reconstruction in which triangle shaped atomic defects in h-BN have resolved successfully. Boron monovacanies are ideally formed and the dominating zig-zag edges are found to be Nitrogen terminated. The smallest triangle is found to be situated at the corner of hexagons which should corresponds to the monovacancy and all the defects have triangle shape with same direction but the triangle shaped holes are found to have discrete size. The Boron monovacancy(V_B) and Nitrogen monovacancy(V_N) should have opposite orientation while (V_B) and (V_{3B+N}) are in same direction surrounded by two co-ordinated Nitrogen atom [8].

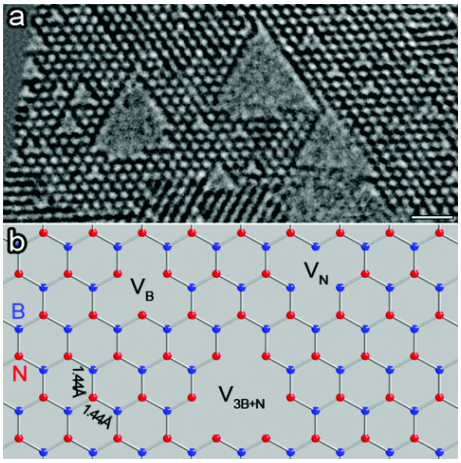

Figure 4.5: (a) Monolayer of h-BN showing monovacancies and larger vacancies and (b) Modes for the atomic defects in h-BN [8].

4.2.2 Energy and Stability

We run the scf input file and got the total energy of our system, the Fermi energy, the Kohn-Sham states, the energy eigen values and the magnetic moment to explain the magnetization along with the forces and stresses on individual atoms. With the help of these available data, we can calculate the defect formation energy for vacant system in

the h-BN sheet. The formula to obtain the defect formation energy (E_F) is,

$$\mathbf{E}_F = (\mathbf{E}_d - \mathbf{E}_p) + \mathbf{n}\mu \tag{4.1}$$

In this equation [35], E_d is the total energy of defected (single vacant) h-BN sheet, E_p is total energy of pristine h-BN sheet, n is the number of Boron or Nitrogen atom removed and μ is the chemical potential of the atom removed to create the vacancy. The chemical potential μ for B and N atoms were calculated using DFT with appropriate pseudopotentials by considering an isolated system of single atom.

Table 4.4: Different energy values required to calculate the formation energy (in Rydbergs; 1 Rydberg = 13.6 eV)

Formation energy of single B vacant h-BN	
Study in system	**Energy (Ry)**
Single Boron vacant h-BN (E_d)	-625.613
Pristine 4x4 h-BN (E_p)	-637.809
Energy of isolated B atom(μ)	-10.986
Formation Energy($\mathbf{E}_F$)	1.21

Formation energy of single Nitrogen vacant h-BN	
Study in system	**Energy (Ry)**
Single Nitrogen vacant h-BN (E_d)	-609.029
Pristine 4x4 h-BN (E_p)	-637.81
Energy of isolated N atom(μ)	-27.835
Formation Energy($\mathbf{E}_F$)	0.944

From above tables it is seen that the defect energy for V_B is -625.613 Ry and that of V_N is -609.029 Ry. Both the system had been relaxed and hence both are stable. Also the defect formation energy E_F for V_N is 0.944 Ry (12.84 eV) and E_F for V_B is 1.21 Ry (16.45 eV). It is found that the defect formation energy for V_N is less than that of V_B. Thus we can say that the single Nitrogen vacant system is more favourable than single Boron vacant system.

4.2.3 Band Structure Calculation

An isolated atom has discrete energy level and the electrons are filled on that levels according to Pauli Exclusion Principle if there is no any perturbation. These discrete energy levels are called atomic orbitals. However, these discrete energy levels can be perturbed by bringing a large number of atoms together. In the presence of any other atom near to the initial atom under consideration, each energy level get splitted into a pair of energy level with narrow width. Consequently, when we brought many number of atoms close to each other to form a molecule, their atomic orbital split into a large number of closely packed discrete molecular orbital. A solid is formed by bringing a large number of atoms together. In such case, a number of orbital becomes very large and hence the difference in energy between the different atomic orbital is very small. In solids the energy levels of electrons form continuous bands of energy rather than the discrete energy levels of the atoms in isolation. Here, we get the continuum level of energy and is called the band.

The energy bands can be empty, filled, forbidden and mixed [36]. A solid can be classified as metal, insulator and semiconductor by studying the nature of the energy bands. A solid is called a insulator if the allowed energy bands are either completely filled or empty and metal are those whose bands are partly filled whereas the semiconductor has one or two bands are slightly filled or slightly empty with band width of nearly 1eV [37]
.
Up to now, the various methods have been utilized to calculate the band structure such as tight binding approximation, nearly free electron approximation, green function approximation, muffintin approximation and so on.

However, we employ density functional theory to calculate the electronic band structure by using quantum espresso code. By using the first brillouin zone we have calculated the entire band structure of our system. The fisrt brillouin zone of the hexagonal lattice with Γ-K-M-Γ high symmetry point is shown in the following figure. Here $\vec{a}$, $\vec{b}$ and $\vec{c}$ are the reciprocal lattice vectors.

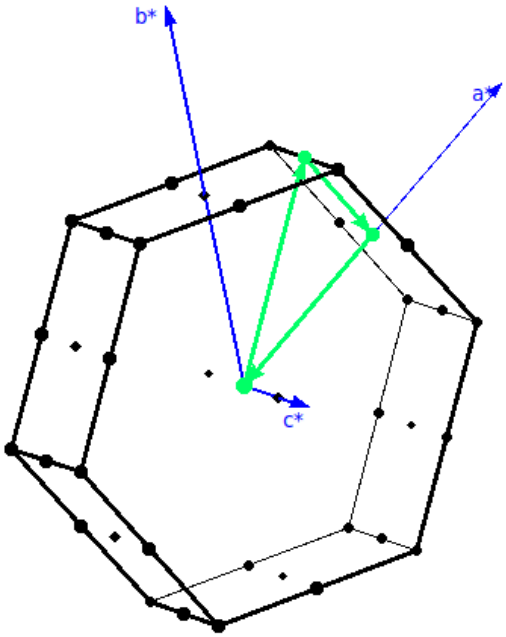

Figure 4.6: First brillouin zone of hexagonal lattice with high symmetric points. We have chosen Γ-M-K-Γ path.

Band Structure of Pure Hexagonal Boron Nitride

Pristine h-BN is an insulator with large band gap as well as a non-magnetic system. While, it's insulating helps in various application in many nano devices. In our work, we made ground-state study of pristine h-BN in primitive cell and 4×4 supercell. Primitive cell of h-BN contains a basis of two atoms: one B atom and one N atom. It has 8 valence electrons. The output of scf calculation performed in Quantum ESPRESSO consists of available Kohn-Sham states corresponding to the k-points of irreducible Brillouin Zone and the bands calculation yields the possible energy states available corresponding to the k-points along the preassigned path. This output file is used for post production and band structure of the material is obtained.

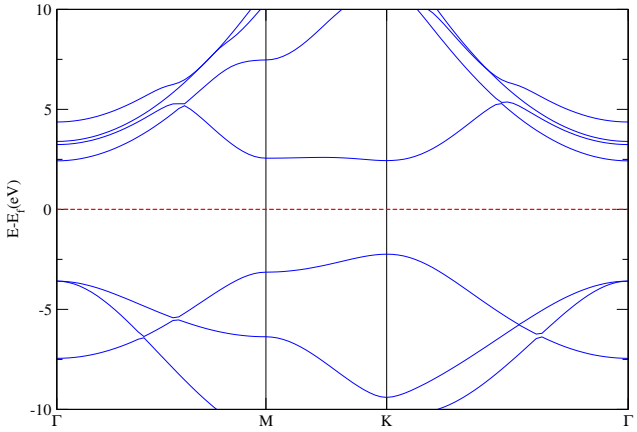

Figure 4.7: Band structure of pristine h-BN using primitive cell, Energies have been measured relative to Fermi energy (E_f = -1.8367 eV).

From this figure, we found that pristine h-BN is a wide gap material with an direct gap, as shown in the above figure. There is a gap of around 4.681 eV along the K-point. Although our study clearly suggest a direct gap, there is much room for possibility of gap being a indirect one. Published results with PBE calculation also confirm an indirect gap of 4.56 eV.

As well as we observed spin-polarised calculations on 4×4 h-BN supercell and obtained the band structures for up-spin and down-spin electrons. The band structures are as below:

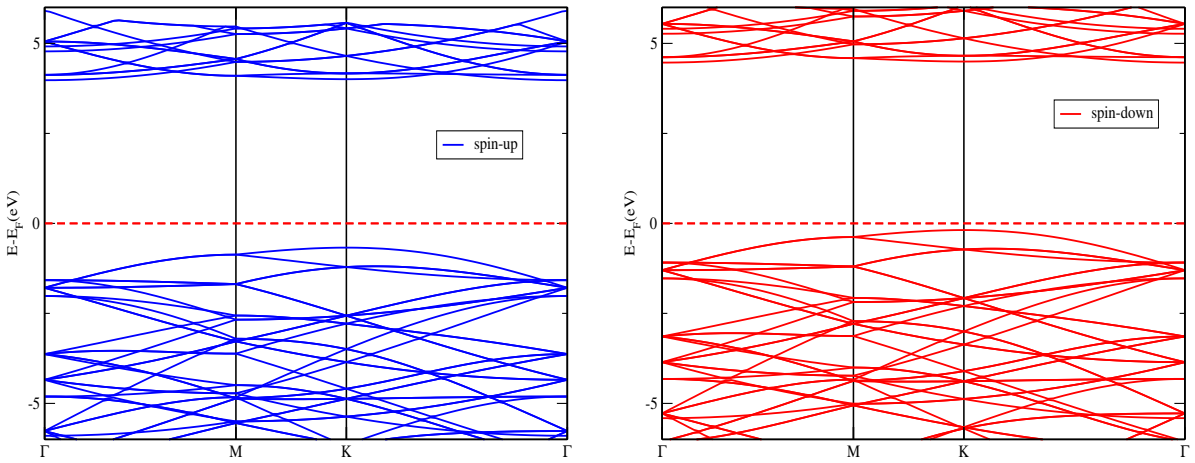

Figure 4.8: Band structures of pristine h-BN using 4×4 supercell , Fermi level (E_f= -4.0162 eV) is set to zero.

From these band structures we see that the arrangement of Kohn-Sham states in reciprocal space is identical for both spins. The band gap is 4.642 eV. Hence showing insulating behaviour. The contradictory nature of gap could be due to folding of band

while calculations are conducted in a supercell.

4.2.4 Density of States and Magnetization

The non magnetic nature of pristine h-BN can be seen from the spin polarised density of states plot. Distribution of available states for both up and down spin is symmetrical so that h-BN is nonmagnetic which can be seen in the figure below.

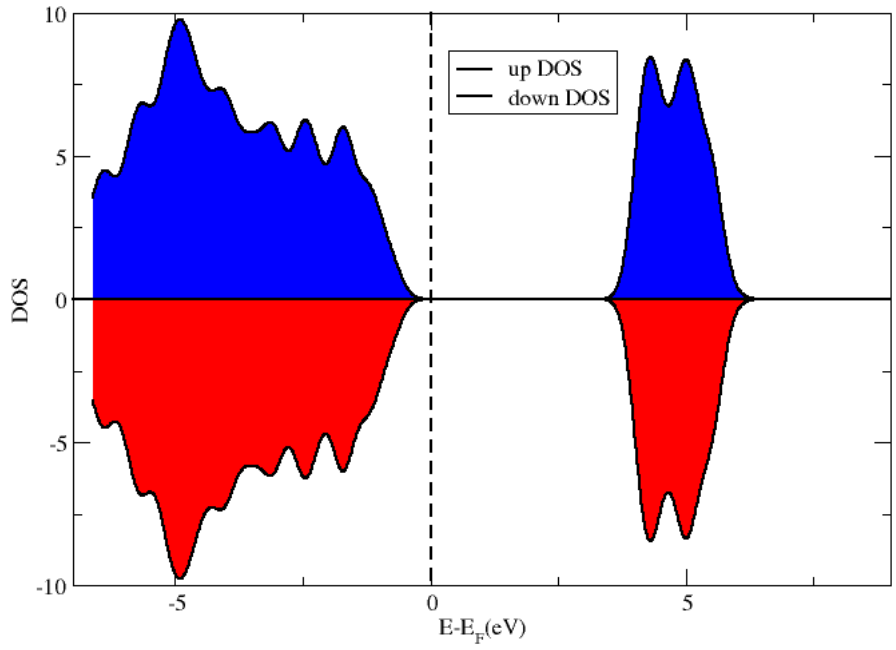

Figure 4.9: Density of States for 4×4 supercell of pristine h-BN.

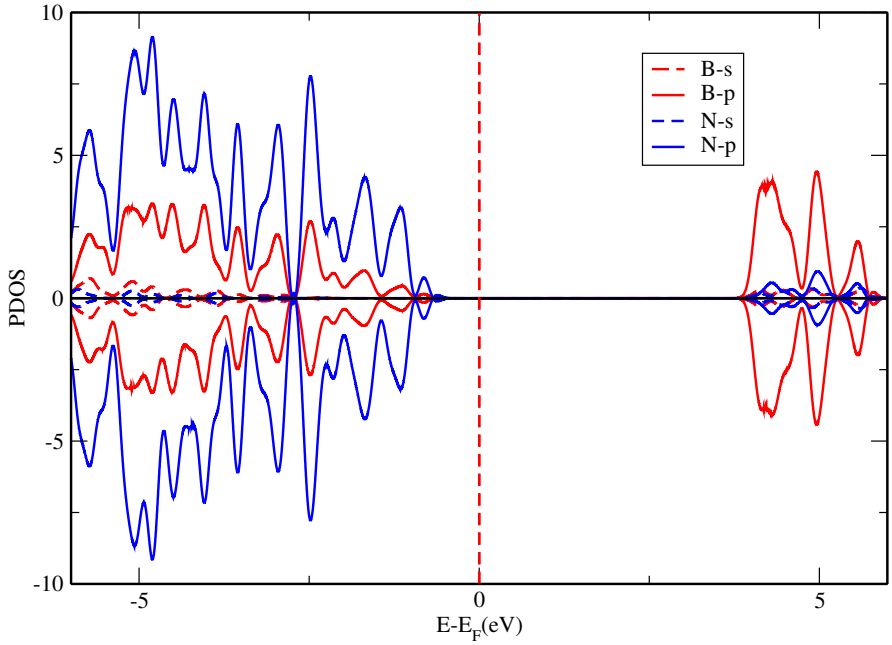

Figure 4.10: PDOS for s and p orbitals of B and N atoms of 4×4 supercell of pristine h-BN.

From above we see that DOS is high in the region where many bands are accumulating and low in the regions where the number of bands lines are less in number. Also the DOS is completely zero in the region where no any bands lines i.e. between the valance and the conduction bands. Below fermi level bands are mainly dominated by 2p orbitals of N atom and above fermi level by 2p-orbitals of B atom.In overall we can say p orbitals are more dominant that s orbitals. The s-states for both B and N atoms are almost absent. Also the DOS for s and p orbitals for both atoms in up spin and down spin state are exactly symmetrical. The pure h-BN is thus a non magnetic meterial whereas creating single vacancy with element like N and B can induce some magnetic moment, which has been discussed below.

4.3 Electronic and Magnetic properties of Monovacant h-BN

On creating vacancy in any material, it can change the electronic as well as magnetic properties of that material. Due to presence of vacancy in h-BN, we observe many changes on its different properties. We also observed significant changes in band structure induced due to vacant system. We studied spin polarized scf, DOS and Projected

DOS calculations on our monovacant system.

4.3.1 Single Boron vacant 4×4 h-BN sheet (V_B)

The following figures show the band structure of single vacant hBN due to V_B. The spin polarised calculations were conducted to see the effect of single vacancy on different spins. We observed that for up spin, electrons are in valance band and touched the Fermi level whereas the spin down electrons in the conduction band are lying 1.4eV above the fermi level. These new states present are due to the effect of vacancy. These bands around the Fermi level are significantly different to those in pristine 4x4 h-BN (figure 4.8). we can say that energy levels of valance orbitals (s and p) of B and N are also changed around the Fermi level. From figure 4.11 we see that when B is removed from h-BN sheet, the system is half metallic in nature with insulating behaviour for up spin and metallic nature for down spin. In this case both up and down spin have direct band gaps of 4.75eV and 1.02eV respectively at the symmetric points Gamma for up spin and K for down spin where the first one lies in the range of band gap of h-BN from 3.0 to 7.5 eV [14].

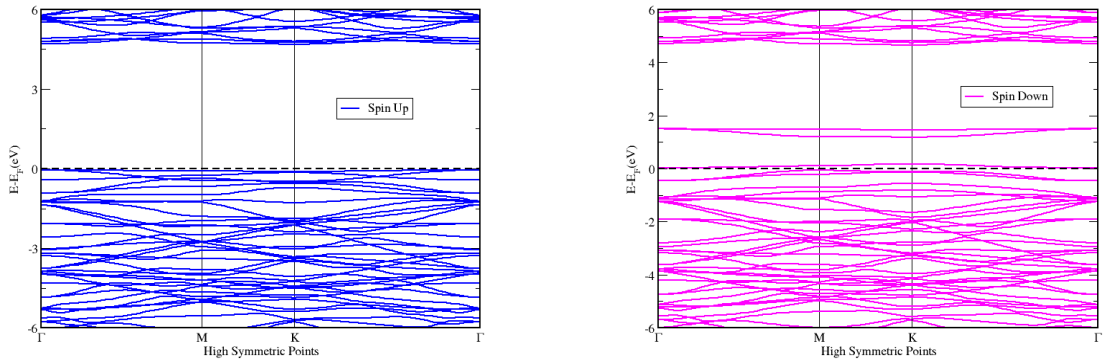

Figure 4.11: Up and Down spin band structures of single Boron vacant h-BN (V_B), Fermi level (E_f= -4.1685 eV) is set to zero.

From above we see that vacancy defect specially influences near about fermi level. The fermi level is shifted down towards occupied state as compared to defect free h-BN. The system changes from nonmagnetic to magnetic half metal with total magnetization is 2.74 μ_B/cell The Fermi energy is equal to -4.1685 eV and this is due to the removal of B atom. Comparing with band structure of primitive h-BN we can understand the states around Fermi level (just above the valence band) must be mainly due to V_B.

4.3.2 Density of States and Magnetization of V_B

The non magnetic nature of pristine h-BN can be seen from the spin polarised density of states plot. Distribution of available states for both up and down spin is asymmetrical so that the monovacant h-BN is magnetic. Furthermore, we can elaborate understanding about above system with help of DOS and PDOS calculations. We present the total DOS and PDOS for V_B as below.

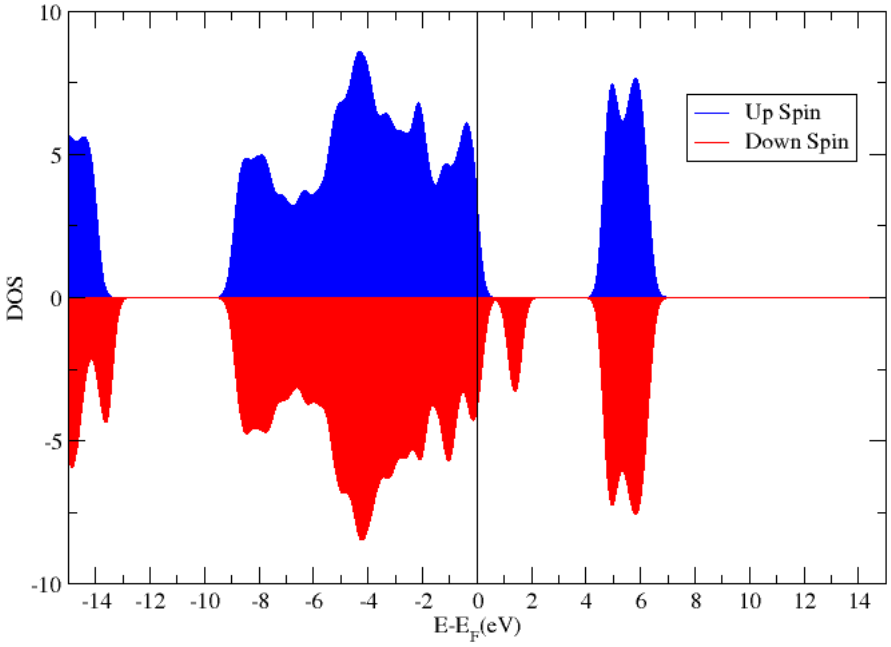

Figure 4.12: Density of states plot for (V_B)

From above figures we see that the DOS plot for up spin and down spin for 4x4 defected supercell are found to be slightly unsymmetric, depicting the magnetic nature with total magnetization of $2.74\mu_B$ for V_B. Thus, this system behaves as magnetic system. In comparison to pristine 4x4 supercell where up and down DOS are symmetric and system behaves as non-magnetic. The individual B and N atom behaves as magnetic materials as they have magnetic moment of $1\mu_B$ and $3\mu_B$ respectively.
To see more closely on the contribution of atomic orbitals of each atom we also have presented and discussed with PDOS plots as shown below.

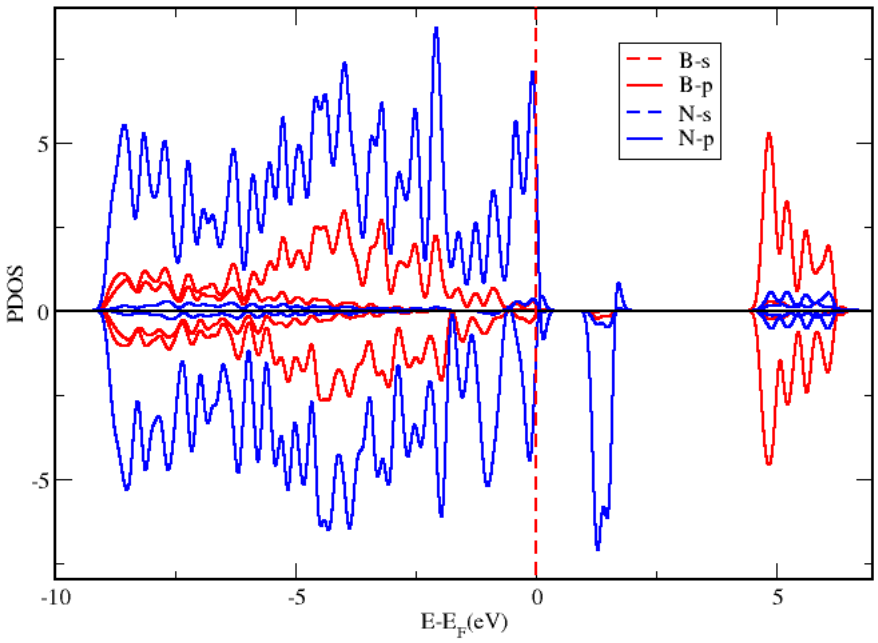

Figure 4.13: Projected Density of States of hBN with (V_B)

From the Projected DOS calculations we see that for h-BN sheet with V_B, the available states around Fermi level are largely due to N and B atom. In both B and N atom, 2p orbitals are more dominant than s orbitals. Due to this the system is magnetic in nature. The contribution of 2p orbitals of B and N atom to the magnetization is relatively greater than 1s orbitals. Below the Fermi level N, 2p orbitals are dominant whereas above Fermi level, 2p orbitals of B atom are significant. For 2p orbital of N atom, we see some contribution just above Fermi level. The system has got magnetic nature with magnetic moment 2.74 μ_B/cell.

4.3.3 Single Nitrogen vacancy in 4×4 h-BN sheet (V_N)

The following figures show the band structure of single vacant hBN due to V_N. We observed that for up spin, electrons are in valance band are lying 0.08eV below Fermi level whereas the spin down electrons in conduction band are lying 0.33 eV above the Fermi level. These new states present are due to the effect of vacancy. These bands around the Fermi level are significantly different to those in pristine 4x4 h-BN (figure 4.8). we can say that energy levels of valance orbitals (s and p) of B and N are also changed around the Fermi level. From figure 4.14 we see that when N is removed from

h-BN sheet, the system is semiconductor in nature as it is semiconductor for up spin and insulator for down spin as seen from figure. In this case both up and down spin have indirect band gaps of 1.44eV and 3.27 eV respectively at the symmetric points K and M for both up and down spin.

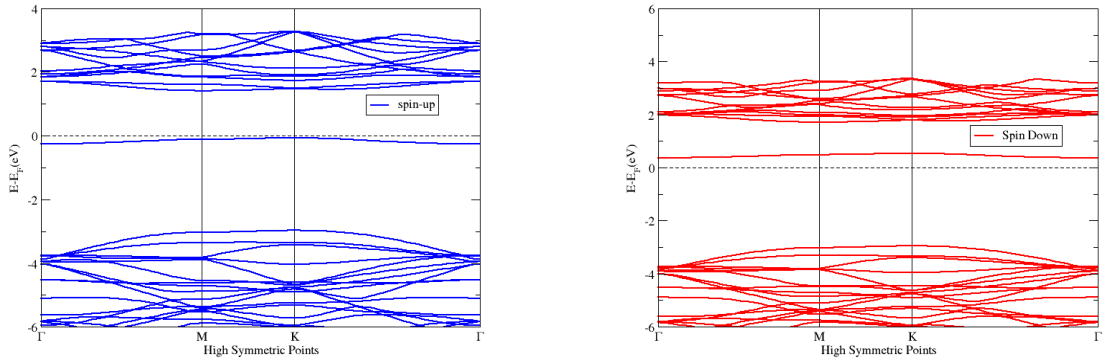

Figure 4.14: Up and Down spin band structures of single Nitrogen vacant h-BN at B site (V_N), Fermi level (E_f= -1.3790 eV) is set to zero.

From above we see that the new energy states created near fermi level. Fermi level is shifted up towards unoccupied state as compared to defect free h-BN. W can say the system changes from nonmagnetic to magnetic semiconductor with total magnetization is 1 μ_B/cell

The Fermi energy is equal to -1.3790 eV and this slight decrease in Fermi energy level is due to the removal of N atom. Comparing with band structure of primitive h-BN we can understand the states around Fermi level (just above the valence band) must be mainly due to V_N.

Chapter 5

Conclusions and Concluding Remarks

We have carried out our research work to investigate the stability, electronic and magnetic properties of pure hexagonal boron nitride due to single vacancy in h-BN sheet. All these calculations have been performed by employing density functional theory under DFT-D_2 level of approximation using generalized gradient approximation(GGA), exchange correlation functional including spin polarized calculations with the use of Quantum espresso package. We have accounted an interaction between the ion cores and the valence electrons with the use of ultrasoft pseudopotential(USSP).

Two dimensional hexagonal Boron Nitride is the most studied layered material after graphene. In forms of nanosheet, nanowire and nanotubes it has been studied for its interesting properties of high thermal conductivity, high chemical stability and insulating properties. Many theoretical and experimental studies employing different computational techniques have concluded that electronic band gap is wide and can be both direct or indirect. Further, owing to the chemical inertness scientist have been studying defected h-BN for possibility of novel electronic and magnetic properties. Hexagonal Boron Nitride has also been called as white graphene due to analogy in its structure with same number of electrons in primitive cell to the it. Accordingly study of vacancy in two dimensional h-BN is interesting for analyzing electronic and magnetic phenomena have been a temptation to scientific community. So far monolayer h-BN with N and B vacancy had not been done in our department till date. We studied structural, electronic and magnetic properties of h-BN sheet due to single B and N vacancy based on first-principles calculations under theoretical framework of Density Functional Theory.

We conducted first-principles calculations using ultrasoft pseudopotentials under Generalised Gradient Approximation with PBE functional for exchange-correlation functional implemented in Quantum ESPRESSO code (version 6.5). We focused on changes in electronic and magnetic properties due to single vacancy in a 4×4 supercell of h-BN. Before running our final calculations we conducted the convergence tests taking a primitive cell. Total energy converged for a cut-off kinetic energy of 45 Rydbergs and for $18 \times 18 \times 1$ mesh of k-points for Brillouin zone sampling. The optimal value of lattice parameter was found to be 4.74 Bohrs. Using these optimized parameters we conducted primitive cell relaxation under BFGS scheme. We created a $4x4$ supercell with help of relaxed primitive cell and removed a B and an N atom in the sheet to create a vacancy. This vacant system was also used for relax calculation until the system attained optimal geometry with minimum energy. Finally, we conducted band structure and DOS, PDOS calculation using these relaxed structures.

The N-B-N and B-N-B bond angle are 123.94 Å and 119.71 Å for V_B and V_N respectively. The nearest neighbor bond angles B-N-B in V_B is nearly 118.23^0 and nearest neighbor bond angles N-B-N is 115.72^0 for V_N. The formation energy of V_B defect is 16.45 eV and the formation energy of V_N defect is 12.84 eV. Larger formation energy implies lesser stability of the system. Therefore, V_N system is more favorable than V_B system. Regarding electronic properties we conclude that pristine h-BN sheet is an insulator with a wide band gap of 4.74 eV which is in agreement to published results. The direct band gap observed for supercell must be due to the folding of bands. Employment of band unfolding techniques could give us more authentic results and this could be further work that can be done to enhance our knowledge about bands and band structure. We also found from spin polarised DOS calculations that pristine h-BN is non magnetic in nature.

We create single vacancy by removing B and N atom one after another. Our study of these two systems (V_B and V_N) reveals that the V_B system is half metallic and V_N system is semiconductor. Additionally,the band gap for up spin electrons in V_B is very high (4.75 eV) but for up spin electrons in V_N the gap significantly less (1.44 eV).Also, the band gap for down spin electrons in V_B is 1.02 eV but for down spin electrons in V_N the gap significantly less (1.16 eV). Further, the DOS and PDOS plot revealed that the vacant system is magnetic and magnetic behaviour is dominant by the p orbital of the atoms. Further,the magnetic nature with total magnetization of $2.74\mu_B$/cell for V_B

and $1.00\mu_B$/cell for V_N. Thus, this system behaves as magnetic system.
Also the B-N bond length around non-defective region and triangular structures for V_B and V_N respectively can be seen physically and are found to be matched with the experimental value as described in the previous chapter.

This work was conducted with limited computational resources compared to the standard and gravity of requirements for first-principles research. A supercell size larger than 4×4 is necessary to study vacant system. Also study of charge density and charge transfer would be more helpful for fruitful analysis.
One can further expand this work in order to study the following properties:

- One can do same research in bilayer hBN
- One can study the charge transfer properties
- One can study the charge density properties
- One can extend this work by taking the higher supercell
- One can do the same research by creating multiple vacancies in both monolayer and bilayer
- One can do the same research by doping other atoms in the vacant system in both monolayer and bilayer
- One can do the same research by creating vacancies in other compounds as well as in larger supercell

References

[1] M. Xu, T. Liang, M. Shi, and H. Chen, Chemical reviews **113**, 3766 (2013).

[2] C. Kittel, *Introduction to Solid State Physics* (Wiley, 2004).

[3] N. Ashcroft and N. Mermin, *Solid State Physics*, 33rd ed., HRW international editions (Holt, Rinehart and Winston, 1976).

[4] W. Bollmann, *Crystal defects and crystalline interfaces* (Springer Science & Business Media, 2012).

[5] M. Petrescu and M.-G. Balint, UPB Sci. Bull., Series B **69**, 35 (2007).

[6] D. Golberg, Y. Bando, Y. Huang, T. Terao, M. Mitome, C. Tang, and C. Zhi, ACS nano **4**, 2979 (2010).

[7] L. Song, L. Ci, H. Lu, P. B. Sorokin, C. Jin, J. Ni, A. G. Kvashnin, D. G. Kvashnin, J. Lou, B. I. Yakobson, *et al.*, Nano letters **10**, 3209 (2010).

[8] C. Jin, F. Lin, K. Suenaga, and S. Iijima, Physical review letters **102**, 195505 (2009).

[9] J. Wang, F. Ma, and M. Sun, RSC Advances **7**, 16801 (2017).

[10] P. Bissokarma, M. Sc. Thesis, Central Department of Physics, Tribhuvan University (2018).

[11] S. Majety, X. Cao, R. Dahal, B. Pantha, J. Li, J. Lin, and H. Jiang, in *Quantum Sensing and Nanophotonic Devices IX*, Vol. 8268 (International Society for Optics and Photonics, 2012) p. 82682R.

[12] B. Huang and H. Lee, Physical Review B **86**, 245406 (2012).

[13] N. Ooi, V. Rajan, J. Gottlieb, Y. Catherine, and J. Adams, Modelling and Simulation in Materials Science and Engineering **14**, 515 (2006).

[14] V. Solozhenko, A. Lazarenko, J.-P. Petitet, and A. Kanaev, Journal of Physics and Chemistry of Solids **62**, 1331 (2001).

[15] H. Wang, Y. Zhao, Y. Xie, X. Ma, and X. Zhang, Journal of Semiconductors **38**, 031003 (2017).

[16] E. Kaxiras *et al.*, *Atomic and electronic structure of solids* (Cambridge University Press, 2003).

[17] E. Fermi, Rend. Accad. Naz. Lincei **6**, 5 (1927).

[18] L. H. Thomas, in *Mathematical Proceedings of the Cambridge Philosophical Society*, Vol. 23 (Cambridge University Press, 1927) pp. 542–548.

[19] S. Kümmel and L. Kronik, Reviews of Modern Physics **80**, 3 (2008).

[20] P. Hohenberg and W. Kohn, Phys. Rev. **136**, B864 (1964).

[21] W. Kohn, Physical Review Letters **76**, 3168 (1996).

[22] D. Sholl and J. A. Steckel, *Density functional theory: a practical introduction* (John Wiley & Sons, 2011).

[23] W. Kohn and L. J. Sham, Physical review **140**, A1133 (1965).

[24] M. P. Marder, *Condensed matter physics* (John Wiley & Sons, 2010).

[25] R. Zeller, Multiscale Simulation Methods in Molecular Sciences (J. Grotendorst, N. Attig, S. Blügel, and D. Marx, eds.) , 121 (2009).

[26] J. Perdew, K. Burke, and M. Ernzerhof, Physical Review Letters **80**, 891 (1998).

[27] S. Grimme, Journal of computational chemistry **27**, 1787 (2006).

[28] M. Piacenza and S. Grimme, Journal of the American Chemical Society **127**, 14841 (2005).

[29] P. Giannozzi, S. Baroni, N. Bonini, M. Calandra, R. Car, C. Cavazzoni, D. Ceresoli, G. L. Chiarotti, M. Cococcioni, I. Dabo, A. D. Corso, S. de Gironcoli, S. Fabris, G. Fratesi, R. Gebauer, U. Gerstmann, C. Gougoussis, A. Kokalj, M. Lazzeri, L. Martin-Samos, N. Marzari, F. Mauri, R. Mazzarello, S. Paolini, A. Pasquarello, L. Paulatto, C. Sbraccia, S. Scandolo, G. Sclauzero, A. P. Seitsonen, A. Smogunov, P. Umari, and R. M. Wentzcovitch, Journal of Physics: Condensed Matter **21**, 395502 (2009).

[30] P. Giannozzi, S. Baroni, N. Bonini, M. Calandra, R. Car, C. Cavazzoni, D. Ceresoli, G. L. Chiarotti, M. Cococcioni, I. Dabo, *et al.*, Journal of physics: Condensed matter **21**, 395502 (2009).

[31] P. Giannozzi, See http://www. quantum-espresso. org and http://www. pwscf. org .

[32] A. Kokalj, Journal of Molecular Graphics and Modelling **17**, 176 (1999).

[33] P. Turner and V. XMGRACE, Center For coastal and land-margin research, oregon graduate institute of science and technology, Beaverton, Ore, USA (2005).

[34] H. J. Monkhorst and J. D. Pack, Physical review B **13**, 5188 (1976).

[35] H. K. Neupane and N. P. Adhikari, Advances in Condensed Matter Physics **2020** (2020).

[36] R. Martin, Cambridge Daw MS, Baskes MI (1984) Phys Rev B **296443** (2004).

[37] C. Kittel and P. McEuen, *Introduction to solid state physics*, Vol. 8 (Wiley New York, 1976).